ADVANCED MATERIALS
www.advmat.de

Biomimetic and Biologically Compliant Soft Architectures via 3D and 4D Assembly Methods: A Perspective

Jay M. Taylor, Haiwen Luan, Jennifer A. Lewis, John A. Rogers,* Ralph G. Nuzzo,* and Paul V. Braun**

Recent progress in soft material chemistry and enabling methods of 3D and 4D fabrication—emerging programmable material designs and associated assembly methods for the construction of complex functional structures—is highlighted. The underlying advances in this science allow the creation of soft material architectures with properties and shapes that programmably vary with time. The ability to control composition from the molecular to the macroscale is highlighted—most notably through examples that focus on biomimetic and biologically compliant soft materials. Such advances, when coupled with the ability to program material structure and properties across multiple scales via microfabrication, 3D printing, or other assembly techniques, give rise to responsive (4D) architectures. The challenges and prospects for progress in this emerging field in terms of its capacities for integrating chemistry, form, and function are described in the context of exemplary soft material systems demonstrating important but heretofore difficult-to-realize biomimetic and biologically compliant behaviors.

1. Introduction

Nature is full of fascinating examples of 3D structures with intricate geometric and compositional complexity. These structures provide organisms with properties and functions that continue to be superior compared to what can be built synthetically. Studying structures found in nature has motivated and will continue to motivate the advancement of 3D fabrication strategies. Progress in this field has seen tremendous growth in recent years and structures that are made with relative ease today, a few decades ago would have seemed impossible. New developments, particularly in the construction of architectures made from soft materials or hybrid structures containing both soft and hard components are continuously emerging. Creation of soft synthetic structures that mimic the properties and functions of biological materials or can interact with, probe, and control living materials continue to drive research in this field.

Here, recent contributions from the literature and our research are highlighted and the reports are used to highlight opportunities and current needs for advances in the chemistry of soft materials in the context of their functional integration into 3D architectures of complex form. The methods considered herein serve to highlight a recent paradigm for heterogeneous integration—methods of 4D fabrication exploiting directed assembly and printing to construct complex functional composite material structures.

J. M. Taylor, P. V. Braun
Department of Materials Science and Engineering
Materials Research Laboratory
Beckman Institute for Advanced Science and Technology
University of Illinois Urbana-Champaign
104 South Goodwin Ave., Urbana, IL 61801, USA
E-mail: pbraun@illinois.edu

H. Luan, J. A. Rogers
Querrey Simpson Institute for Bioelectronics
Northwestern University
Evanston, IL 60208, USA
E-mail: jrogers@northwestern.edu

J. A. Lewis
John A. Paulson School of Engineering and Applied Sciences
Wyss Institute for Biologically Inspired Engineering
Harvard University
29 Oxford Street, Cambridge, MA 02138, USA
E-mail: jalewis@seas.harvard.edu

The ORCID identification number(s) for the author(s) of this article can be found under https://doi.org/10.1002/adma.202108391.

DOI: 10.1002/adma.202108391

J. A. Rogers
Departments of Materials Science and Engineering
Biomedical Engineering
Neurological Surgery
Chemistry
Mechanical Engineering
Electrical and Computer Engineering
Northwestern University
Evanston, IL 60208, USA

R. G. Nuzzo, P. V. Braun
Department of Chemistry
University of Illinois Urbana-Champaign
600 S Mathews Avenue, Urbana, IL 61801, USA
E-mail: r-nuzzo@illinois.edu

R. G. Nuzzo
Surface and Corrosion Science
School of Engineering Sciences in Chemistry
Biotechnology and Health
KTH Royal Institute of Technology
Drottning Kristinasväg 51, Stockholm 10044, Sweden

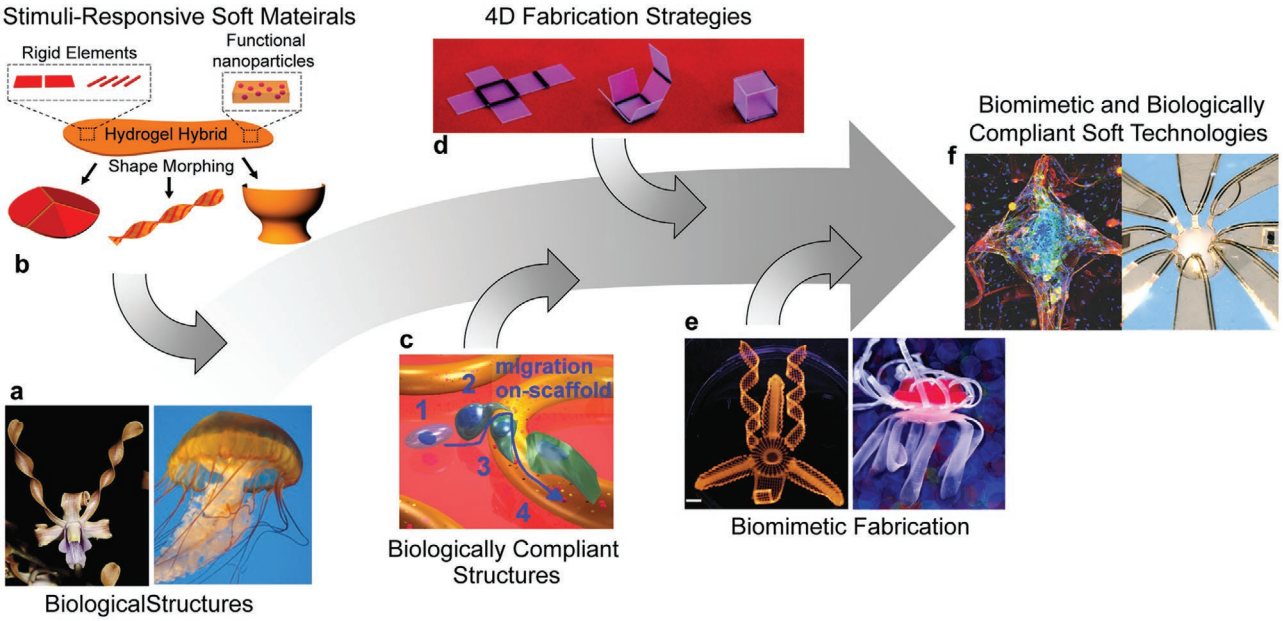

Figure 1. Perspective overview, building biomimetic and biologically compliant structures of sophisticated structure and function requires the culmination of knowledge from many fields. a) Photographs of an orchid flower, *Dendrobium helix*, and sea jelly, *Chrysaora fuscescens*. b) Schematic of deformations seen in shape-morphing hydrogels. c) Schematic of 3D printed structures with biologically compliant chemistry, where the numbers illustrate sequence of motion onto a filament. d) Example of 4D fabrication of polymer sheet into a 3D cube. e) Examples of the fabrication biomimetic structures of a lotus flower and sea jelly. f) Examples of biomimetic and biologically compliant soft architectures that will be presented hererin. a) Left: Adapted with permission.[52] Copyright 2016, Springer Nature. Right: Adapted with permission.[64] Copyright 2019, Wiley-VCH. b) Adapted with permission.[98] Copyright 2017, American Chemical Society. c) Adapted with permission.[122] Copyright 2018, Wiley-VCH. d) Adapted with permission.[17] Copyright 2011, Royal Society of Chemistry. e) Adapted with permission.[52] Copyright 2016, Springer Nature. f) Adapted with permission.[122] Copyright 2018, Wiley-VCH.

Using examples from the literature and our research, exemplary illustrations of such material-based hierarchies of scale and function are shown in **Figure 1**. Our discussion will specifically highlight composite systems integrating soft materials that demonstrate exemplary forms of biomimetic and biologically compliant behaviors, illustrating how design principles can be developed to engender interesting attributes of both form and function in such structures. Of interest to this discussion are the ways chemistries for soft materials fabrication by 3D assembly/printing can be tailored to embed temporal (4D) responses that can be actuated by various means—most notably via mechanisms arising either autonomously in response to physicochemical cues or in programmatic behaviors elicited by the environments of their use.

In recent years, there has been much focus on the development of 4D fabrication strategies. The central focus of these methods is first building an object of simple geometric complexity, then applying a stimulus to reconfigure the object into a more complex form. This strategy has largely been discussed in the field of 3D printing, where a simple, typically planar, geometry is printed, and then a stimulus reforms this geometry into one of higher complexity (i.e., 4D printing).[1,2] This technique has been applied to create many technologies and architectures of sophisticated form and function, which has popularized its use in fabricating 3D soft structures.[3–5]

This concept of first fabricating a simple geometric structure and then using a stimulus to transform it into one of higher complexity has been applied to fabrication techniques outside of 3D printing. One of the first iterations of this type of assembly was seen when a thin planar metal film was evaporated onto an elastomeric substrate. After this deposition and subsequent cooling, the deposited film began to buckle out-of-plane, forming a wrinkled microstructure.[6] Further iterations of this technique have enabled remarkable control and prediction of the buckling patterns[7,8] and have been applied to a number of applications (i.e., controlled wettability,[9] reconfigurable optics,[8,10] and stretchable electronics).[11] We will discuss an extension of this type of assembly in a later section.

Another method of 4D fabrication that has been widely used is the self-folding of polymer films (i.e., soft origami).[12] This type of assembly has been applied in many ways.[13] A simple iteration is the folding of polymer bilayers. In this method, two polymers are combined and reacted to a stimulus. Each layer responds differently to the stimulus and the bilayer bends into a structure defined by its geometry and its mechanical properties.[14,15] Additionally, this 2D to 3D folding of planar polymer films can be achieved through various top-down patterning techniques.[16] One example of this type of patterning is the deposition of ink onto planar polystyrene sheets.[17] When irradiated with light, the ink heats the polystyrene, causing localized contraction and transformation of its structure based on the pattern the ink (Figure 1d). The fabrication techniques of rolled-up nanotechnology[18] and bio-origami[19] apply similar principles to micro- and nanoscale architectures. An extension of polymer folding is seen in the rapidly growing field of soft robotics, where the controlled bending of polymer films is used to grab, transport, and manipulate objects.[17,20]

Another interesting iteration of 4D fabrication is in the assembly of stimuli-responsive micro-/nanoparticles and droplets.[21] Inspired by the assembly of proteins, nucleic acids, and other biomolecules found in nature, this method uses synthetic particles and dynamic self-assembly to build and disassemble nanoscale and microscale structures. There are many great reviews that summarize this growing field, which shows promise in applications in controlling chemical reactions and nanoparticle therapeutics.[22]

Aiding in the design and development of many of the described 4D fabrication strategies is the use of computational tools, such as finite element analysis (FEA).[15,23–26] These tools allow researchers to predict precisely how the fabricated structure is likely to reconfigure upon triggering. This becomes crucial in the design of sophisticated 3D geometries necessary for the advanced applications described later in this perspective. The use of optimization tools (e.g., machine learning) has recently shown promise in streamlining the design and fabrication process and is now being used to help construct customized and advanced structures.[23,27] We strongly suspect use of these optimization algorithms will continue to grow in popularity, particularly, as these fabrication methods become ever more utilized for industrial applications.

The abovementioned strategies of 4D fabrication have shown tremendous potential in creating soft materials with the kinds of complex form and function seen in biological systems. From here on, we will focus specifically on the development of two 4D strategies: direct ink writing (DIW) and directed assembly through compressive buckling. In particular, we want to show the progress we have made on using these methods to mimic the form and function of biological systems and show how we can integrate these structures with living cells and tissues to control their maturation and growth. We will discuss these examples in the context of both opportunities and remaining challenges of these methods. In the end, we will lay out specific challenges to and opportunities of 4D methods in future technologies.

2. 3D/4D Printing of Soft Matter

3D printing is a ubiquitous method for rapidly designing and fabricating soft materials for a myriad of applications,[28–30] including soft electronics,[31] sensors,[32] stimuli-responsive actuators,[33,34] soft robotics,[35–37] and vascularized human tissues.[38] One of the principal advantages of 3D printing is that it enables planar and 3D architectures to be patterned with controlled composition and structure across a range of length scales spanning from hundreds of nanometers to 1 m or larger.[39] Ink chemistries are tailored to simultaneously satisfy requirements for printability as well as the desired materials properties in the final fabricated structure.[29,40–42] Stereolithography, Digital Light Processing, and DIW serve as important exemplars of 3D printing methods, each harboring specific advantages as a means of 3D fabrication and having different requirements to achieve high print speed and resolution.[28] Of these, DIW enables a broad range of soft material chemistries including hydrogels,[3,40] polymer composites,[43,44] emulsions,[45,46] and elastomers,[47] to be fabricated into biomimetic and biologically compliant designs. Recent advances in multimaterial core–shell structures[48] and multinozzle printheads[36,49,50] serve to further enhance the programmable compositional and geometric complexity that can be achieved by DIW.[2,36,51]

The ability to pattern stimuli-responsive soft materials has ushered in a new patterning method, known as 4D printing, in which the initially defined composition and shape in the x–y–z dimensions evolves over time in response to external stimuli.[2–4,37,52,53] One approach for the heterogeneous integration and patterning of soft composite structures that encode the desired 4D temporal response is multimaterial DIW. This intricate programming allows a material to selectively respond to external stimuli either through a direct change in the material properties in response to the stimuli or indirectly, through a series of reactions catalyzed by the stimuli. It is this paradigm of hierarchy and functional integration that we feel best defines 4D printing as a distinct class of 3D fabrication. The literature now describes some striking examples of 4D printed structures that display dynamic forms of programmed functionality.[37,43,54–57] These include examples of shape reconfiguration (e.g., Figure 1b) and other forms of dynamics in response to external stimuli—humidity,[52] temperature,[33,58] light,[59,60] pH,[61] osmotic forces,[62] electromagnetic fields,[54,63] and flow[64] (e.g., Figure 1d)—with high selectivity due to their underlying programming of chemomechanical properties.[33,59,65] Soft materials can thus be printed with high spatial resolution in the quiescent state, which respond "on demand." Complex responses, such as the directed evolution of an object's morphological shape (e.g., Figure 1b,d) or directed integration of living cells (e.g., Figure 1c,f) have been demonstrated to date. The desired response is achieved via carefully controlling the ink chemistry and print path to encode anisotropic properties that stem from their molecular to microscale structure, yet manifest at the macroscope scales in 2D to 3D or 3D to 3D' shape changes over time.

A particularly striking example of 4D printing involves printing a cellulose-fibril-filled hydrogel ink in a planar bilayer design, which folds into a complex 3D biomimetic orchid shape upon swelling (Figure 1e).[52] Mechanics models established a deterministic print path to encode the desired stiffness and, hence, swelling anisotropy needed to drive complex forms of 3D mean and Gaussian curvature. Through inverse design, soft composite architectures can be pattered in planar motifs, which subsequently "bloom" over time akin to the 3D hydronastic shape transformations of a flower.[52] The use of osmotic forces is not a limiting feature, since other mechanisms can be used to elicit the gradients in properties required to drive bending, twisting, and ruffling.[53,66,67] As recently demonstrated, this approach can be extended to systems driven by thermally induced phase transformations, embedded prestrains, shape-memory materials, or selective wetting.[5,33,43,57,67]

The adoption of 4D printing as a tool to build intricate 3D structures has grown tremendously in popularity. Along with soft responsive hydrogels, this technique has been demonstrated with other types materials, including rigid plastics,[58,68] polymer composites,[43,44,69] elastomers,[37,55,70] shape-memory polymers,[5,67,71] and biomaterials containing living cells and tissues.[72] This last example, 4D bioprinting, specifically has shown tremendous promise in many healthcare applications.[73,74]

The temporal aspect of this technique is either applied to mean manipulating living organisms using stimuli-responsive architectures or using 3D printed structures to control the maturation and growth of living cells and tissues.[73] The latter case is the form of temporal response that we will target in the examples in the coming sections.

3. Directed 4D Assembly by Compressive Buckling

Directed assembly of complex 3D mesoscopic architectures by compressive buckling represents another promising approach for fabricating functional 3D structural forms of materials.[25,75] Guided by analytical and numerical modeling techniques, controlled compressive buckling drives the transformation of photolithographically patterned planar thin-film materials into diverse yet predictable 3D geometries.[25] In this context, 2D thin-film precursor structures are firmly bonded, via covalent bonds, at selective anchor locations (which we refer to as bonding sites) to a prestretched elastomeric substrates, the stress relaxation of which induces compression imparted onto the 2D precursors through bonding sites and drives the controlled buckling and associated 2D to 3D transformation. The directed 3D assembly approach maintains full compatibility with advanced planar semiconductor technologies, works seamlessly with nearly all classes of thin film materials (e.g., semiconductors, polymers, and metals), applies to wide-ranging characteristic length scales ranging from hundreds of nanometers to centimeters, and operates in a high-throughput, parallel fashion.

The use of this technique in creating functional 3D structures has expanded in recent years.[76–78] Successful demonstrations of directed 3D assembly have been applied to many applications, including electronics/optoelectronics with unconventional form factors,[25,79] microelectromechanical systems,[80] energy harvesters,[81] cell scaffolds,[76,82,83] multifunctional interfaces to organoids,[84] electronic microfliers,[85] microfluidic networks,[78] and many others.

Introducing 4D capability (i.e., temporal evolution) into the directed 3D assembly enables appealing, additional control over the morphology and functionality of the material system. One evident advantage of the 3D structures developed by directed assembly lies in the reversible control on the degree of 2D to 3D geometric change by simply stretching/releasing the underlying elastomeric substrate, which is a pristine form of 4D shape evolution. Controlling other factors such as the degree of prestrain or the number of axes in which compression is applied (i.e., uniaxial, biaxial, equiaxial) can also affect the final structure. Also, in many instances, the assembled structure has different properties (i.e., electrical,[79,86] magnetic,[87] biocompatibility,[76] etc.) compared to the preassembled planar structure. Advances in design concepts further equip the directed 3D assembly approach with various 4D capacities of programmable temporal shape changes. For example, multistable buckling mechanics enables morphable 3D mesostructures to reversibly switch between multiple (e.g., two to four) 3D geometries by changing the time sequence of stress relaxation of a biaxially stretched elastomer substrate;[79,88] incorporating transient constituent materials and/or responsive materials (e.g., shape-memory polymers) into the 2D precursor structures leads to programmable shape changes in the resultant 3D systems, as a form of 4D electronics;[89,90] besides the 2D/3D structures, shape-memory effects can be introduced to the elastomeric substrates for "on-demand," remotely triggered shape morphing.[26] Furthermore, modeling can provide detailed designs for using strain release to guide the assembly of 3D material mesostructures.[25,78,79,81,90,91]

When biologically compliant soft material chemistries are interfaced with the 2D precursors prior to assembly, the assembled structure can be used to support living cells. Early examples of this form of hierarchical 3D assembly illustrate the functional integration of a 4D ink microstructure by DIW on top of and in registry with the planar precursor of a single-crystalline Si 3D mesostructure (**Figure 2**a). Release of strain in the supporting substrate drives the formation of nested and truncated helical structures combining the functional chemistry of a soft gel material in hierarchy with the morphology of the silicon 3D mesostructure (Figure 2b). In combination, the fabrication methods make it possible to couple the compositional and biologically compliant forms of function associated with soft materials with those provided by state-of-the-art electronic/photonic/optoelectronic materials. In the current work, the control capacities of 4D fabrication provide a route to integrate surface chemistries to support complex cellular assembly on a supporting mesostructure scaffold embedding other forms of function (vide infra).[76]

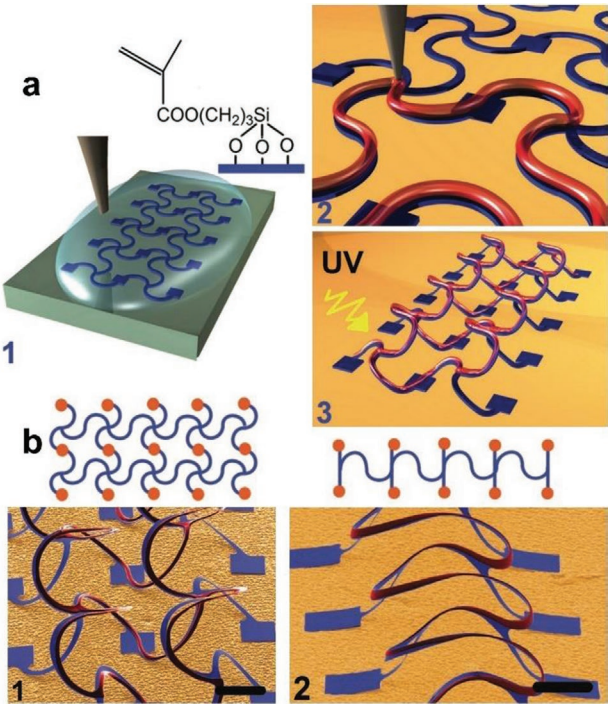

Figure 2. a) Schematic for integration of methacrylate ink on 3D mesostructure via DIW, 1) ink adhesion surface treatment, 2) ink microstructure by DIW on top of planar precursor, 3) ink UV cure on buckled mesostructured. b) Schematic (contact pads bound to substrate—orange, scaffold—blue) and colorized scanning electron microscopy (SEM) images (substrate—yellow, scaffold—blue, methacrylate gel—red) (scale bar = 200 μm). a,b) Adapted with permission.[76] Copyright 2017, Wiley-VCH.

4. Biomimetic 4D Fabrication of Soft Materials

The ability to design and fabricate soft and living materials with more complex 4D responses is an open challenge. Future progress will require the development of material systems whose mechanics can support heretofore difficult-to-realize attributes of dynamical performance (e.g., fast, reversible, large amplitude motions). A grand challenge involves locally programming the material response in an autonomic manner, which living organisms demonstrate ubiquitously. Through the heterogeneous integration of dissimilar soft materials, we embodied the desired physicochemical and mechanical properties necessary to mimic flexural dynamics (i.e., the speed and type of the motion) observed in Echinoderm and Cnidarian organisms ("sea jellies," **Figure 3**a–c).[64] This example highlights the development of broadly tunable ionotropic hydrogels that allow construction of systems that replicate critical features of the motions exhibited by these creatures. For example, two structurally similar objects were 3D printed with different compositions in targeted domains of the final biomechanically mimetic structure. Each composition was chosen to directly pattern gradients of mechanical properties within the 3D printed objects. Specifically, we leveraged an ionotropic (alginate-based) composition for these hydrogels, adding targeted additives (e.g., polysaccharides, nanoclays, and polyvalent anions and cations) in gradient form to control print rheology, mass transport, and mechanical properties within the distinct spatial domains of the patterned objects. The rich compositional characteristics of these systems allowed us to develop broadly tunable and robustly patternable DIW inks. By developing these inks at two levels of design—one to control the 3D shape evolution on immersion in water and the other to provide a hierarchy of flexural rigidity—it is possible to support a broad range of responses, as driven by the local attributes of flow fields, created by the ionic gradients programmed into the printed object (Figure 3a,b). This is most directly exemplified in the forms adopted by the exumbrella tentacles (Figure 3c) that, based on osmotic pressure differences created by the valency of the ion-binding agent, either are flexible and curl upward (divalent—calcium, Figure 3c1) or remain planar and extend outward (trivalent—iron Figure 3c2). The anisotropies and the low moduli of the tentacles impart a gradient condition to their flexibility as well, allowing it to move dynamically in a current of water in a way that closely resembles the natural creature it mimics.

Another strategy to achieve localized response of a soft materials is to combine the responsive polymers with hard thin-film

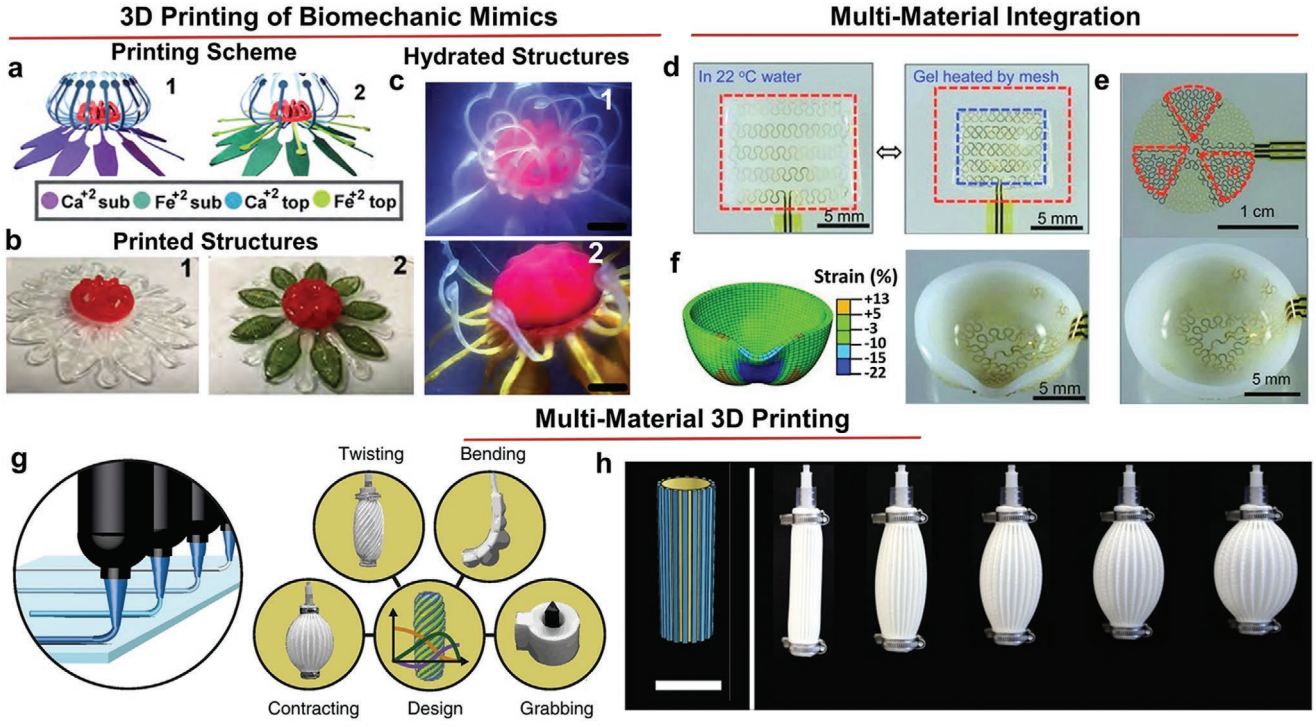

Figure 3. a) Schematic of two targeted biomimetic structures, where different colors highlighted in inset represent ink chemistries that dynamically move in water and red represents soft polymer formulated for structural rigidity. b) Photographs of the as-printed structures and c) of the hydrated structures (left scale bar = 35 mm, right scale bar = 8 mm). a–c) Adapted with permission.[64] Copyright 2019, Wiley-VCH. d) Photographs of Joule heating structure embedded into a thermoresponsive hydrogel before and after current is passed to raise gel temperature and cause contraction. e) Photographs of segmented Joule heating mesh and of the mesh embedded into a hydrogel structure. f) FEA and the corresponding optical image of the deformation of the segmented mesh hydrogel when one segment is heated. d–f) Adapted with permission.[92] Copyright 2013, Wiley VCH. g) Schematic of multimaterial 3D printing being used to create soft actuators capable of 4 different motion types. h) Schematic and photographs of device consisting of stiff stripes printed on a soft inner tube that is subsequently pressurized to deform structure (scale bar = 2 cm). g,h) Adapted under the terms of the CC-BY Creative Commons Attribution 4.0 International license (https://creativecommons.org/licenses/by/4.0).[96] Copyright 2018, The Authors, published by Springer Nature.

materials in the form of stretchable/flexible geometric layouts, following mechanics models to afford each with the desired/programmable features of mechanical performance. The hard material components can be fabricated using precise lithographic techniques and tailored for properties (e.g., electrical, thermal, etc.) that can interact with the soft material without altering its chemistry. Here, we will show one example of this hybrid structure that will foreshadow some of the more sophisticated examples of this strategy that will appear later in this perspective.

In the example of interest, a stretchable Joule heating electrode mesh is embedded into a thermoresponsive hydrogel (Figure 3d).[92] When a current passes through the mesh electrode, the temperature increases, causing the hydrogel to undergo a lower critical solution temperature (LCST) phase change that results in the hydrogel contracting. The mesh is fabricated in a mechanically compliant geometry that allows it to deform with the hydrogel without constraining its motion. Due to the pure elastic mechanics of the electrode mesh and the hydrogel, the driven strains of this actuator are fully reversible, with the initial state recovered when the temperature of the hydrogel returns below the LCST transition.

An advantage to this strategy is that the heating electrode mesh can be patterned to localized regions of the hydrogel and be independently addressed to impact its swelling behaviors to effect programmable forms of flexural shape morphing.[92] This is illustrated by an exemplary hydrogel network with three separately addressable mesh segments embedded within a hemispherical hydrogel shell (Figure 3e). Applications of current to differentially heat the mesh segments make it possible to locally drive flexural shape morphing of the hydrogel in distinct programmable ways that are in turn quantitatively predicted by a finite-element model of the device (Figure 3f).[92]

The ability to integrate materials with various mechanical properties seamlessly into a single structure has also been explored extensively in multimaterial 3D printing.[4,53,93] In this field, composite structures,[43,44] the use of multiple nozzles,[36,50,94] and hierarchical design principles[45,95] have been used to create functional materials with structures that mimic those found in natural organisms. Here, we highlight one example, in which silicone inks formulated to have different stiffnesses were used to create biomimetic soft actuators.[96] The inks were printed into architectures that underwent programmed deformations based on their pattern of soft and stiff silicone filaments. When pressurized, the architectures would deform in four distinct motions, contracting, twisting, bending, or grabbing (Figure 3g). In one example, a single layer of the soft silicone (Figure 3h, yellow region) is first printed on top of a rotating cylindrical support and then a stiffer silicone is printed in filaments that run parallel to the first layer (Figure 3h, blue region). The presence of the stiffer filaments constricts the motion of the architecture, resulting in contraction of the material (Figure 3h). A similar approach of integrating soft and stiff silicone inks is used to create actuator structures with other motions.

Taken together, the results highlighted in Figure 3 suggest an opportunity to develop even more empowering chemistries for 4D fabrication that might provide transformations between programmable states of shape and form. An extension of this concept is to focus on chemical responses within soft polymers that lead to local changes in the material structure.

5. Development of Responsive Chemistries for Efficient Photomechanical Transduction

Specifically, an area that would expand many applications in 4D assembly is to focus on materials that can be reconfigured through interactions with light. There are many reviews that describe photoresponsive chemistries[97] and their use in 3D fabrication methods.[42,57,98] Polymers can be made photoactive by doping them with a compound that heats the material when irradiated with light,[99] causing a phase change that reforms its shape. Photoactive polymers can also be made by adding a chemical that will undergo an isomerization reaction when light of a certain wavelength is absorbed (e.g., azobenzenes[100] and spiropyrans[60,101]) or they contain a photocatalyst that will initiate a reaction that leads to the shape change.[102,103] Many of these chemistries are not efficient when it comes to converting light energy to mechanical work. We feel that there is a particular need to develop chemistries compatible with 4D fabrication techniques that are capable of efficiently converting light to mechanical work.

Light in many ways would be an ideal stimulus for 4D fabrication techniques, it has high spatial and temporal precision and provides the opportunity for rapid and localized transformation of the material chemistry and structure using a remote source (**Figure 4**a).[104] Herein, we highlight two exemplars from our past work that demonstrate such forms of photoresponsiveness, and that we think illustrates the broader prospects necessary to develop new polymeric systems capable of efficiently converting light energy to mechanical work via coupled mechanisms of photo-chemomechanical transduction.

In the first example (Figure 4b), the incident light initiates a photocatalytic reaction cascade that induces a change in the pH of the local aqueous environment in which the hydrogel material is placed. This gradient in pH is harnessed to drive the chemomechanical actuation of the material system.[102] Through careful study of this system, and applying the quantitative features of the thermodynamic models that govern its mechanical response, we can identify key features necessary to create high efficiency photo-chemomechanical systems.[102] Namely, these features are to: i) rely on efficient and reversible reactions; ii) use sustainable forms of mass transport within the material; iii) minimize the resistance of inactive layers to mechanical motion; and iv) to reduce the diffusion of reactive species responsible for the mechanical work. To help achieve these requirements, it is apparent that advances in 3D fabrication methods that are capable of heterogeneous integration of functional components are necessary in developing such high-efficiency material systems.

In the second example, light is used to form dynamic and reversible cross-links within a polymer (Figure 4c). Specifically, light alters the state of a spiropyran photoisomer polymerized within the structure. In one state, the spiropyran is neutrally charged and shows little interaction with metal ions also present in the polymer matrix. When exposed to UV irradiation or heat, the spiropyran isomerizes to the charged merocyanine form and multiple merocyanines coordinate to each of the metal ions present in the matrix (Figure 4d). These metal-centered cross-links

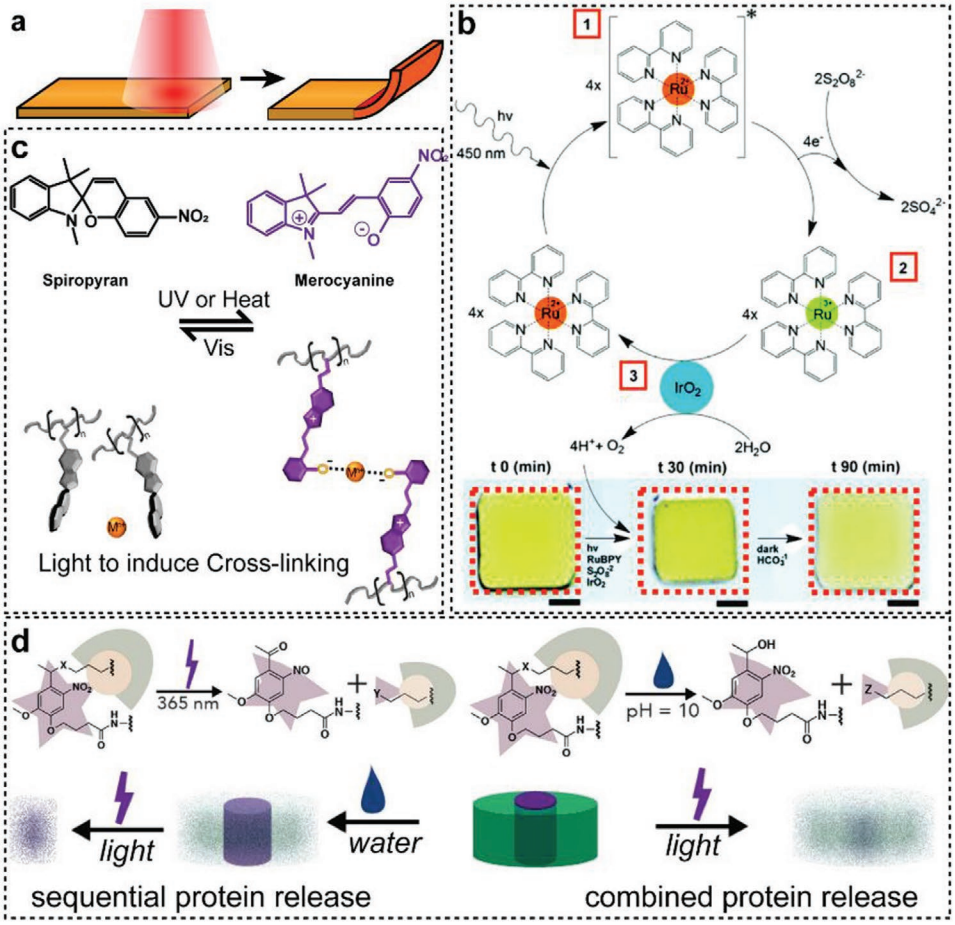

Figure 4. a) Schematic of localized deformation when light is irradiated onto a soft sample source. b) Reaction scheme of a photocatalytic chemistry embedded into a soft hydrogel material that lowers the pH of the system, resulting in the reversible contraction of the soft hydrogel. b) Adapted with permission.[102] Copyright 2017, Royal Society of Chemistry. c) Schematic of the photoisomerization of the spiropyran (SP) group into merocyanine (MC), showing an example of how reversible light-induced cross-linking can affect a material's mechanical properties. Adapted with permission.[105] Copyright 2019, American Chemical Society. d) Schematic of multicomponent hydrogels comprising photolabile chemistries. The hydrogel consists of nitrobenzyl moieties with various labile bonds, X that will alter the degradation of the gel. The combination of hydrogels made with different labile bonds allows proteins to be released from the gel both in sequence and in combination. Adapted with permission.[109] Copyright 2020, American Chemical Society.

significantly alter the mechanical properties of the polymer. When measured, the polymer's storage and loss modulus increase by more than an order of magnitude as a result of this photoisomerization.[105] Upon application of visible light, the merocyanine converts back to the spiropyran form, and the cross-links disappear.

Though neither of these first two examples are direct applications of 4D fabrication, they illustrate reversible light-responsive chemistries that are capable of performing mechanical work within a soft material using a stimulus external to the soft material. The concept of using remote sources to manipulate soft materials, we think, could be transformational in building future technologies at the biology/material interface.

In line with this concept are the compelling ways in which photodegradable hydrogels have been used in technologies to control living cells.[106,107] Popular in this field is the use of nitrobenzyl or coumarin groups as the photolabile cross-linkers.[108] These groups will cleave when irradiated with light and will soften the hydrogel as well as release cargo trapped within its structure. In one example of these types of polymers, nitrobenzyl moieties featuring four different types of labile bonds (e.g., ester, amide, carbonate, and carbamate, Figure 4d) were synthesized and their photolytic and hydrolytic properties were studied.[109] Of these four labile bonds, the carbamate moiety showed the slowest rate of hydrolysis and superior light responsiveness under physiological conditions. More so, the combination of hydrogels cross-linked with different types of labile bonds was used to show the release of proteins both sequentially and in combination (Figure 4d). This type of demonstration would have applications in many technologies including drug delivery,[110] tunable cell scaffolds,[106,111] and responsive biomaterials.[112] The continued development of soft material chemistries capable of photoreversible and 4D structural change would enable the next generation of these applications.

6. Tuning Biological Compliance of 3D Printed Soft Material Scaffolds to Control Cellular Response

Hydrogel materials have played an important role as substrates for model cellular microcultures. Recent progress has made it possible to use these materials as supporting scaffolds for the complex 3D organization of cells.[113] Many methods are now available that make it possible to pattern these materials with a variety of 3D form factors, including electrospinning,[114,115] electrohydrodynamic jet printing,[116] micromolding,[115,117] and stereolithography.[118] These methods compliment chemical approaches, both synthetic- and processing-based, that yield architectures embedding varying forms of porosity and compositionally sensitive modifications of mechanical properties.[119] Our work in this area has focused on DIW because of its exceptional ability to provide well-controlled 3D spatial, geometric, and physicochemical cues in printed hydrogels that can be further exploited to enhance cell migration, networking, elongation/alignment, and more extended tissue mimetic development.[120–122]

Following this motivation, we have specifically studied 3D hydrogel scaffolds composed of poly(2-hydroxyethyl-methacrylate) (pHEMA), a material that in many ways provides a blank canvas for studies of cellular attachment and growth. As prepared, pHEMA scaffolds demonstrate little activity toward either the promotion or inhibition of cellular dynamics in culture.[121] It is possible, though, to bias this innate agnostic quality. Modifications of the ink chemistry to tune its mechanical and physicochemical properties as well as the addition of specific proteins, peptide-modified proteins, and composite fillers all afford means to modulate growth compliance—to render substrates purposefully between inhibitory and strongly promotive states.[76,121,122] The character of these impacts is strongly cell-type-dependent, although important general trends do emerge.

For instance, we found that by changing the homopolymer-to-monomer (Mr) ratios in the ink before printing (**Figure 5**a), we can prepare physicochemically distinct pHEMA gels (pHH-1 through pHH-4)[121] that after subsequent modification with poly-L-lysine (pLL), a common additive for increasing cell growth compliance, can regulate cell growth properties. The Mr ratio effects the physical cross-link density and the overall mesh architecture and ultimately how pLL can bind (tenaciously absorbing via multivalent intersegmental hydrogen bonding interactions) to the 3D printed material (Figure 5b). The mesh of the gel serves to directly modulate the spatial distribution of cationic charge carried by the pLL.

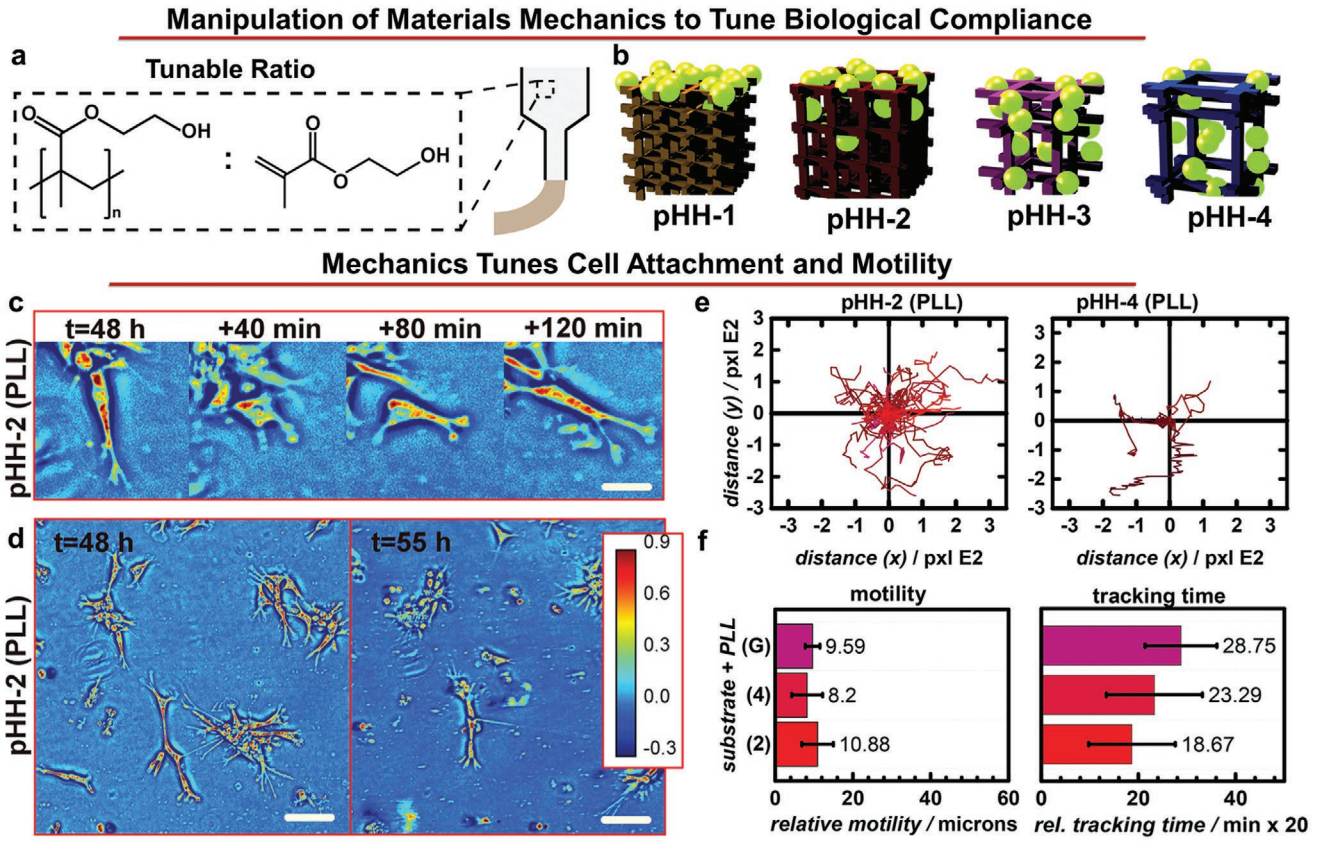

Figure 5. a) Schematic of the monomer ratio of the ink prior to printing and b) the resultant pHEMA gels that were printed (pHH-1–4), showing that the differences in mesh densities effect the absorption of pLL protein (yellow spheres). c) Spatial light interference microscopy (SLIM) images of 3T3 fibroblast single cells (scale bar = 28 μm). d) SLIM for representative cell culture region of 3T3 at 48 and 55 h (scale bar = 100 μm). e) 3T3 cells' relative motility data on pHH-2 and pHH-4 substrates (scale factor = 1.59 pixel μm^{-1}). f) 3T3 relative motility and tracking quantification for glass (G), pHH-2, (2), and pHH-4 (4) substrates. b–f) Adapted with permission.[121] Copyright 2016, Wiley-VCH.

For optimum cellular growth, a balance must be kept between migration and attachment, which are connected to the elastic modulus and surface energy of the substrate. As cross-linking density increased, so did the elastic modulus but the surface energy, as measured by atomic force microscopy, decreased.[121] Cell cultures seeded on these four mesh architectures showed differences in growth compliance and cellular motility resulting from these physiochemical differences. We tracked the attachment and motility of the 3T3 cells on pHH-2 and pHH-4 substrates (Figure 5e) and found that significant levels of growth compliance were evidenced only on the pHH-2 substrate, where the 3T3 cells are seen to move within and between cellular clusters. By contrast, the 3T3 cells tended to be immobile and did not attach viably to the pHH-4 substrate, resulting in a lack of formation of cellular networks. This difference in substrate behavior is further exemplified in the relative motility and tracking quantification data (Figure 5f), where in general, the 3T3 cells had higher motility and stayed in the field of view for shorter times on the pHH-2 substrates compared to pHH-4 substrates. We also note in this work that the behaviors of the E1 preosteoblasts were also tracked using the same methodology and were found to have similar results on the pHH-2 and pHH-4 substrates, indicating that the observed behavior is not specific to one cell type. The differences in substrate viability seen between these cell types directly correlate with the behaviors found in cultures conducted on more complex substrates. The physicochemical attributes of the inks are directly exploited in the sections that follow to illustrate the unique ways that these 3D microcultures can guide the maturation and motility of cells over time leading to their targeted 4D behavior.[121]

The previous example, and current literature,[123] provide strong guidance as to the mechanisms that can be exploited to create programmable 4D behaviors of biologically compliant architectures. More specifically, the broader body of this work illustrates the tunable qualities that the incorporation of additives can confer to both the growth compliance and the material mechanical properties. Alone, the use of protein surface treatments makes it challenging to pattern features of cellular integration and growth at fine hierarchical scales. The use of a broader range of mechanical and physiochemical additives in 3D printable pHEMA inks, however, can enable 4D patterning of more complex forms of growth compliance and cellular integration.[122]

In one example, we used two pHEMA inks—the first one affording little affinity for mediating cell attachment and a second that as a result of a specific viscosity modifying agent does so strongly. We printed a complementary sequence of serpentine gel filaments supported on a base gel substrate composed of each type of ink (**Figure 6**a).[122] In the one case, we used an ink closely related to the chemistry of those presented in Figure 5. This ink is composed of a composite pHEMA gel doped with Laponite, a smectite clay (LHi) (Laponite is a trademark of the company BYK Additives Ltd.). Structures printed with this ink were paired with those derived from a pHEMA composition (pHH) with low cell viability. In cultures carried

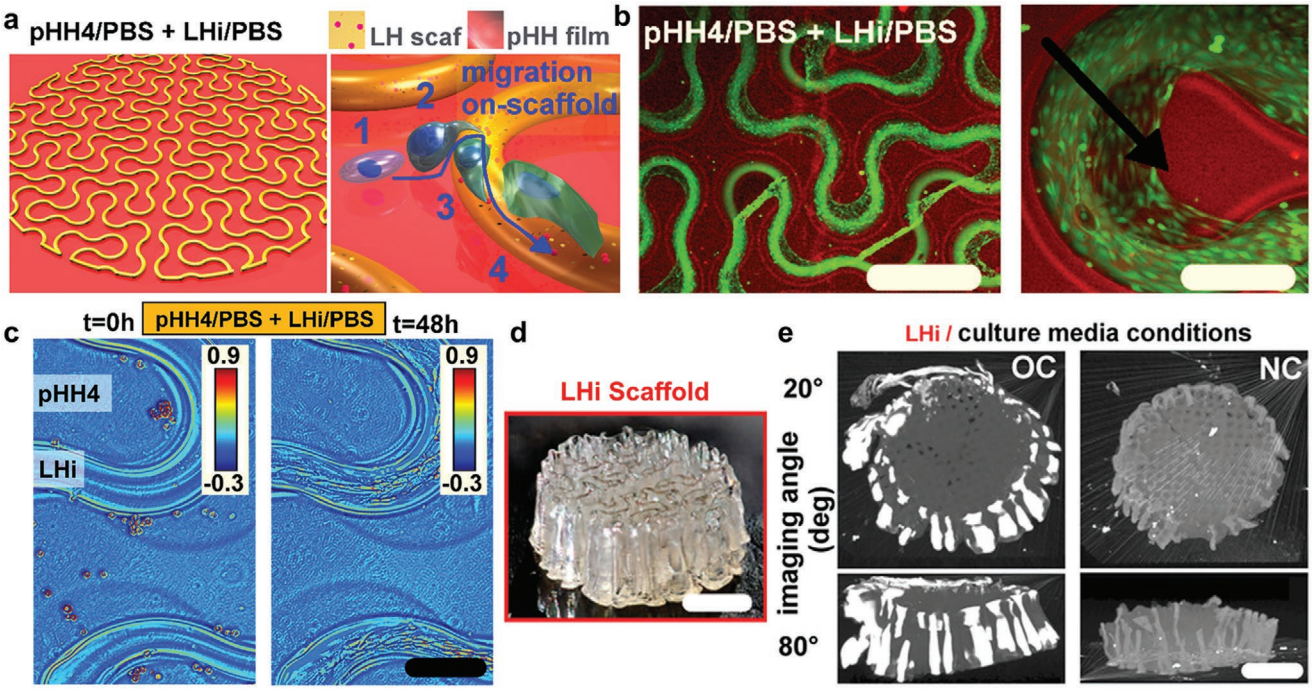

Figure 6. a) Schematic of pHH-4 films patterned with LHi filaments and incubated in phosphate-buffered saline (PBS) to induce cells to attach to the regions with higher biological compliance. b) Live/dead cell assay of 3T3 fibroblast cells on the printed architecture where green represents living cells and red represents dead cells (left scale bar = 600 µm, right scale bar = 150 µm). c) SLIM image of cellular attachment and migration 3T3 cells initially with spherical cell moving and spreading on the LHi filaments after 48 h (scale bar = 120 µm). d) Macroporous 3D structure of a LHi scaffold as-printed (scale bar = 3 mm) and e) X-ray microtomographic images after culturing E1 preosteoblasts in osteoconductive (OC) or non-osteoconductive (NC) media (scale bar = 3 mm). a–e) Adapted with permission.[122] Copyright 2019, Wiley-VCH.

out using 3T3 fibroblasts, two distinct cell attachment and migration behaviors were found for both cell types. Irrespective of its placement (whether as the filament or substrate), the Laponite/pHEMA composition always comes to dominate within the culture as the preferred point for cellular attachment and proliferation (Figure 6a, here shown as the filament). Those cells contacting pHH regions initially exhibit poor attachment and spherical morphologies and over time migrate to the interface between the pHH film and LHi substrate. This is exemplified in a live/dead cell assay (Figure 6b), where the living cells (green) are almost exclusively on the LHi filament and the dead cells (red) are present almost exclusively on the pHH film. These features are also seen in excerpts taken from spatial light interference microscopy (SLIM) data (Figure 6c), which tracks cell responses on LHi–pHH substrates over the first 48 h of time in culture. As seen in Figure 6c, round cell bodies are observed initially on the edges of the LHi filament, and then migrate to the LHi filament after 48 h. This same trend holds when the filament and substrate chemistries are reversed. These data strongly establish that 4D growth compliance is effectively "self-directed" to LHi areas of the scaffold.[122]

The selective attachment and growth of cells illustrated in the examples above are ones that are retained and dominate growth on more complex 3D structures and as well as impact subsequent 4D development. For instance, when a macroporous structure fabricated using an LHi composition is seeded with E1 preosteoblast cells (Figure 6d) and subsequently cultured in osteoconductive media, a cellular differentiation occurs that results in strong on-scaffold localizations of biogenic mineralization (Figure 6e). In this case, the white contrast in an X-ray microtomographic images shows the formation of biogenic apatite that occurs predominantly on the exterior walls of the scaffold. The data further suggest that, at the scale of the scaffold shown, the limitation of diffusion of species through the internal macroporous structure inhibits cellular proliferation to deep regions within it, but vascularization would sustain cells more viably throughout the scaffold. It should be noted that control cultures carried out in non-osteoconductive media do not generate similarly mineralized scaffolds.[122] Overall, these examples show the control that has been developed through the use of tailored materials chemistry for the 4D scaffolds.

In these examples, we show how cell adhesion and proliferation can be controlled by tuning the physiochemical properties of the ink used in the 3D printed structure. Our strategy was to control the homopolymer-to-monomer ratio of the ink, which controls the physical properties of the ink, and then perform a surface chemical modification over the entire structure using poly-L-lysine. This combination of control led to the differences in cell adhesion and migration seen in our printed structures. There are many other examples in the current literature where tuning the physiochemical nature of a biomaterial surface is used to control cellular adhesion, proliferation, and differentiation.[124] The ability to modify material surfaces in this manner has led to some remarkable developments in many applications.[125] The continued focus on developing surface chemical modification strategies to locally tune the pattern and density of modifying agents will continue to be an opportunity for future research efforts.

7. 4D μ-Cellular Frameworks Fabricated through Directed Assembly for Monitoring and Regulation of Biological Tissue

Finally, we highlight portions of a broader body of collaborative work that examines the use of mechanics to drive complex forms of 3D assembly for 4D function. In an exemplary case, a new material chemistry was examined to regulate cell interactions occurring within a 3D mesostructured scaffold. Here, we investigated the directed assembly of model multicellular structures associated with the peripheral nervous system—the dorsal root ganglion (DRG)—using an arginine–glycine–aspartic acid (RGD)-peptide-modified poly-D-lysine (RGD–PDL) to mediate specific integration with a 3D mesostructural scaffold (**Figure 7**a–c). This combination of 3D assembled structure and biocompatibility produces a new form of mesostructure, which we will call 4D μ-cellular frameworks (μ-CFs).[76] This chemistry can be used to broadly tune cellular attachment to the scaffold in ways that mimic integrin-mediated binding to extracellular matrix proteins. The larger results of this and several related studies established that the RGD–PDL when used either as an additive to a pHEMA ink for DIW or a subsequent ab(ad)sorption modifier will direct multicellular assembly in model 4D microcultures. The synthesis of RGD–PDL protein is reasonably straightforward and can be accomplished by using a bifunctional coupling agent to conjugate cystine-modified RGD peptides (cyclic or linear) to the γ-lysine amino groups of the PDL (Figure 7c).[120]

DRG is a neuronal tissue comprising three main cell types (here dissociated from explants of adult rats): 1) the DRG neurons; 2) satellite glial cells; and 3) Schwann cells (Figure 7a). We explored the reconstruction of DRG-like structures from these cellular explants on 4D μ-CFs, using them to direct their organizations in ways that are not possible in traditional 2D microcultures.[76] DRGs formed on two exemplary designs for supporting μ-CFs, one consisting of single-crystalline silicon and the other an SU-8 epoxy (both activated toward cell attachment using RGD–PDL, Figure 7d–g). While the different material properties of the substrates have little apparent effect on the cellular morphologies seen, the larger body of data suggest that marked sensitivities to feature dimensions do exist. The ganglion-mimetic structures grown on a minitable scaffold (Figure 7c) show all three cell types of the explants after ≈45 days in culture. An optical live-cell microscopy image of the latter culture supported on Si (Figure 7d) shows dense fibular bundles due to axonal interconnections between different regions of the scaffold. Calcein-AM live-cell staining (Figure 7e) affirmed the robust viability of these cultures after this extended period postexcision. Two representative images were taken of the μ-CFs with immunocytochemical (ICC) staining specific to neurite (Figure 7f,g), where red represents microtubule-associated protein, green shows glial fibrillary acidic protein, and blue the nucleus. Due to the staining, a green halo (glial satellite cells) is in evidence around the neuronal cell bodies (red arrows in Figure 7f). Networks, mediated by glia, are interconnected between both adjacent and opposite legs of the μ-CF, in contrast to the neurons that aggregate primarily on (and around) its legs. It is notable that DRG-mimetic organizations were not observed in concurrently conducted

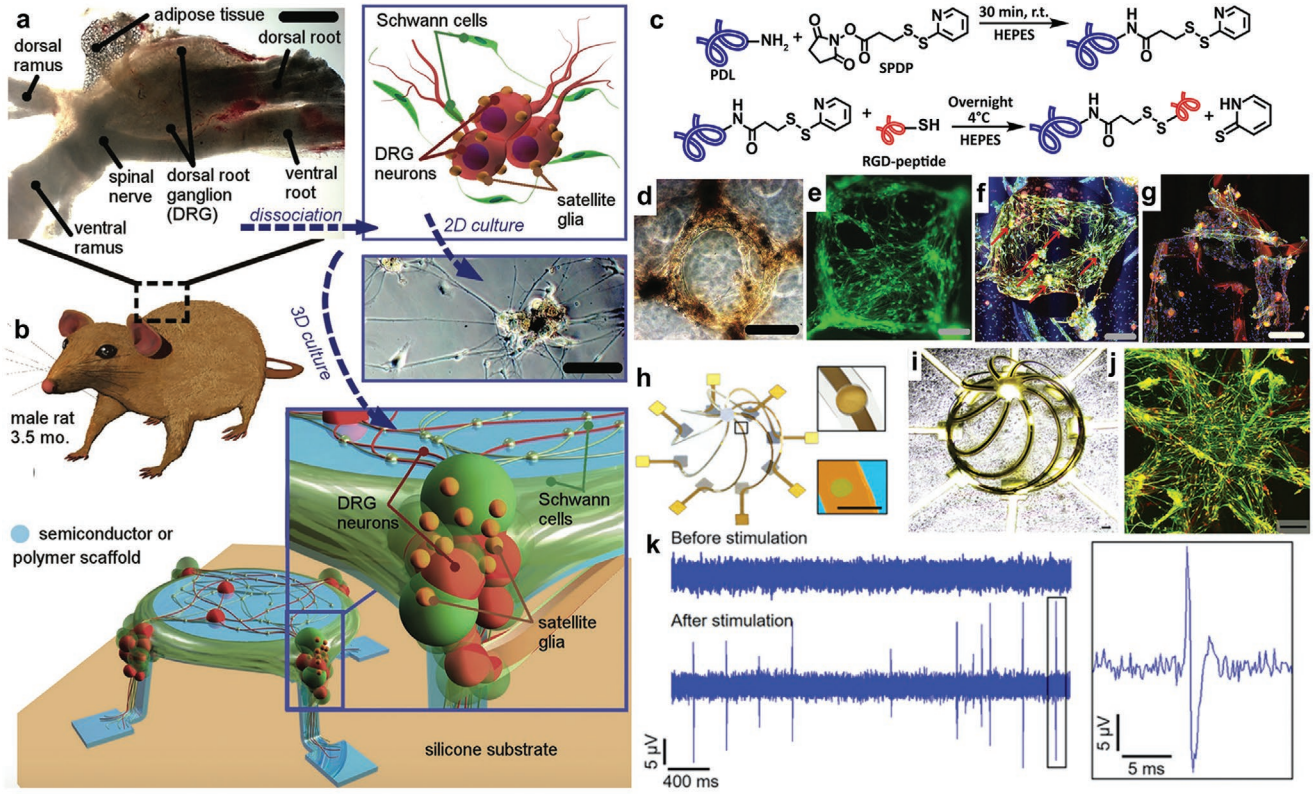

Figure 7. a) Adult rat dissection (scale bar = 450 μm) and dissociation of dorsal root ganglia (DRG) with illustrated components and cell culture (scale bar = 65 μm). b) Schematic of DRG directed growth on buckled mesostructured table array (open or closed top) cultured with DRG. c) Synthesis of RGD-PDL protein. d) Optical phase-contrast microscopy image of buckled mesostructured table array (scale bar = 500 μm). e) Live culture with calcein-AM stain of μ-CF table array cultured with DRG (scale bar = 100 μm), f,g) fixed culture with immunocytochemical (ICC) stain (neurons—red, glia—green, nuclei—blue) (scale bar = 150 μm and 400 μm). h) Schematic and i) optical image of cage mesostructure with eight integrated and separately addressable electrodes for stimulation and recording (scale bar = 100 μm). j) Confocal fluorescence microscopy with immunostaining (neurons—red:antiMAP2, glia—green: antiGFAP) of mesostructure cultured with DRG (scale bar = 100 μm). k) Electrical action potential spectrum before (top left) and after (full—bottom left, magnified—right) electrical stimulation. a,b,d–g) Adapted with permission.[76] Copyright 2017, Wiley-VCH. c) Adapted with permission.[120] Copyright 2017, American Chemical Society. h–k) Adapted with permission.[83] Copyright 2017, The Authors, published by National Academy of Sciences USA.

2D controls, further illustrating the broader potential that 3D (and 4D) scaffold designs may hold for mediating complex forms of cellular network formation.[76]

The work summarized above aided the design of a more highly functional μ-CF, one that allowed for the direct integration of high-precision and high-sensitivity electrophysiological measurement capabilities for the monitoring of the DRG-mimetic networks as they evolved over time in culture. In this study, a μ-CF design of a nested cage with a table-top-like summit was fabricated, one that integrated a series of TiN-coated Au microelectrodes that form the electrode contacts with the cells (Figure 7h). The latter modification promotes high-fidelity electrophysiological measurements in vitro (Figure 7i). As before, an RGD–PDL film was used to provide biological compliance to the μ-CF scaffold and promote attachment of the explant cells. The evolution of DRG-mimetic multicellular organizations occurs progressively with time, their presence being revealed again by direct live-cell imaging studies and detailed assignments from ICC staining (Figure 7j). Electrophysiological responses are not seen promptly in this microculture but, instead, develop over time. An example of the latter, as measured after several days in culture, is shown in Figure 7k. For seven days following seeding and culturing DRG neurons, silent phase states (no measurable signals) prevailed. Stimulating the neurons with a biphasic periodic voltage (frequency: 100 Hz, amplitude: 10 V, duration: 1 s) leads to capacitive charging in the electrode–electrolyte double layer, and subsequent detection of current spikes (bottom left frame of Figure 7k). Magnified views (right frame) show that the spikes have a triphasic waveform, with durations of ≈4 ms and amplitudes between 5 and 16 μV (values consistent with those found in more conventional electrophysiological measurements).[83]

The μ-CFs discussed above illustrate a more general opportunity for the development of assembly-based methods of 4D fabrication. There now exists a growing body of literature that demonstrates the impactful foundations that 4D electronic scaffolds—specifically, as hierarchical devices with well-controlled microelectrode distributions and diverse, precisely defined 3D geometries—can contribute to enhance the control and regulation of tissue formation and function across a variety of biological tissue.[82,126]

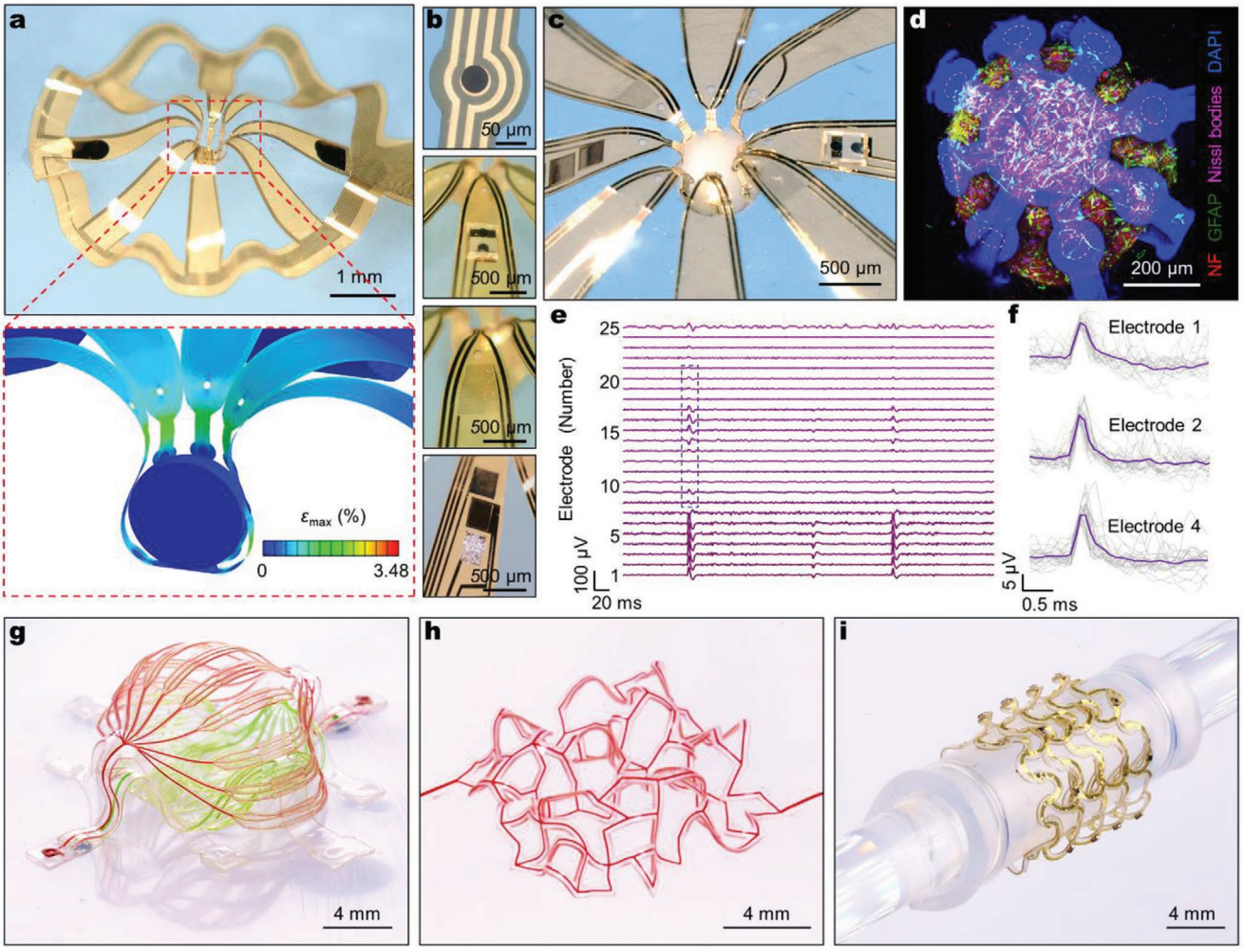

Figure 8. a) Optical image of a compliant, 3D multifunctional mesostructure framework (MMF), with 25 electrodes, as an interface to a neural spheroid (top) and a FEA contour showing the strain across the 3D mesostructure and the neural spheroid (bottom). b) Circular microelectrode (Pt black, diameter 50 μm), μ-ILED, thermal actuator and sensor (Au trace in a serpentine geometry), and electrochemical oxygen sensor (Pt Black, Au, and Ag/AgCl as working, counter, reference electrodes, respectively). c) Optical image of a cortical spheroid enclosed in a 3D MMF designed for electrophysiological recording. d) Confocal microscopy of the spheroid in a similar 3D mesostructure, made of a transparent polymer (parylene-C) without microelectrodes or interconnections; neurofilament (red), GFAP (green), Nissl bodies (magenta), 4',6-diamidino-2-phenylindole (DAPI) nuclear stain (blue), and autofluorescence from the parylene-C (blue). The dashed circles indicate the approximate positions of microelectrodes in a corresponding functional system. e) 3D spatiotemporal mapping of spontaneous neural activity across the surface of a spheroid, with representative field potentials recorded from all 25 microelectrodes in the system. f) Overlay plots of 30 spikes from channels 1, 2, and 4. a–f) Reproduced with permission.[84] Copyright 2021, The Authors, published by AAAS. Reprinted/adapted from ref. [84]. © The Authors, some rights reserved; exclusive licensee American Association for the Advancement of Science. Distributed under a Creative Commons Attribution NonCommercial License 4.0 (CC BY-NC) http://creativecommons.org/licenses/by-nc/4.0/. g) Optical image of a double-layer 3D microvascular system formed by mechanically guided assembly. The narrowest microfluidic channel branches have widths of 10 μm, comparable to the sizes of capillaries in human vasculature. h) Optical image of a geometrically irregular 3D microvascular network by compressive buckling. i) Optical image of a 3D hybrid microfluidic and electronic system as an interconnected 4-by-4 double-floor helical microfluidic array with integrated electronic sensors and actuators (e.g., μ-ILEDs, heaters and thermistors, and electrodes). The soft, stretchable hybrid system was wrapped around a glass rod. g–i) Reproduced with permission.[78] Copyright 2021, The Authors, published by AAAS. Reprinted/adapted from ref. [78]. © The Authors, some rights reserved; exclusive licensee American Association for the Advancement of Science. Distributed under a Creative Commons Attribution NonCommercial License 4.0 (CC BY-NC) http://creativecommons.org/licenses/by-nc/4.0/.

In another work, 3D multifunctional mesostructure frameworks (MMFs) serve as compliant neural interfaces to cortical spheroids, which are sub-millimeter-scale constructs of neural cells, and can reproduce complex features of the brain in vitro (**Figure 8**a).[84] These 3D MMFs are important platforms for studies of neurodevelopment and neurological disease modeling using cortical spheroids. Electrical, optical, chemical, and thermal interfaces to cortical spheroids demonstrate some of the capabilities (Figure 8b). The 3D MMF can gently enclose a cortical spheroid, guided by theoretical modeling and design, for high-fidelity electrophysiological recording (Figure 8c,d). The spreading of coordinated bursting events across the surface of an isolated cortical spheroid (Figure 8e,f) and of the cascade of processes associated with formation and regrowth

of bridging tissues across a pair of such spheroids can be spatiotemporally mapped by microelectrodes allocated in the 3D volumetric spaces, which represent some of the unique capabilities of the 3D MMFs tailored for basic neuroscience research.

Artificial microvascular structures represent another important aspect of our efforts to advance 4D μ-cellular frameworks for interfacing with biological tissues. A recent work introduces a directed assembly approach to fabricate complex 3D microvascular structures, by compressive buckling, from 2D microfluidic precursors and integrated devices which are prepared using well-established procedures in 2D micro-/nanofabrication.[78] The resulting microchannels, reservoirs, and valves can be constructed with feature sizes in the micrometer range (e.g., 4 μm in channel width) using the transparent elastomer poly(dimethylsiloxane). This 3D assembly approach in 3D microfluidics offers capabilities in high-resolution features, large area coverage, diverse geometrical layouts, and, as a unique feature, the ability to integrate active functionality through embedded sensors and actuators. Figure 8g demonstrates a double-layer 3D microvascular system formed by mechanically directed assembly. An enclosed internal cavity deterministically forms between the top and bottom layers after compressive buckling. The 3D microfluidic structure features a three-level branching structure and a stepwise change in the width of microchannel (from 100, to 30, to 10 and then back to 30 and 100 μm). The narrowest microfluidic channel branches have widths of 10 μm, comparable to the sizes of capillaries in human vasculature. Additionally, geometrically irregular 3D microfluidic architectures are fully accessible through compressive buckling of the corresponding 2D shapes, e.g., a random 3D network in Figure 8h. Multifunctional platforms that include components for sensing and actuating fluid flows, light exposure, or thermal/electrical stimuli create additional possibilities in 4D μ-cellular frameworks. Figure 8i shows a 3D hybrid microfluidic and electronic system in the form of an interconnected 4-by-4 double-floor helical array of 3D microvascular networks with integrated electronic components (micro-integrated-LEDs (μ-ILEDs), heaters and thermistors, and microelectrodes). Integration of these high-performance electronic components into complex 3D microfluidic architectures leads to systematic microvascular networks with both fluid transporting and electronic sensing and regulating capabilities. The soft mechanics and the open-framework geometries of these systems allow for introduction of biological or nonbiological materials into the open spaces as hybrid configurations that are relevant in engineered tissues and artificial organs.

8. Conclusion: Challenges and Future Opportunities

When taken together, the results presented above illustrate some of the emerging capabilities that functional 4D material structures—ones constructed by using increasingly sophisticated methods of 4D fabrication—are providing and the progress being made in research that exploits them in interdisciplinary contexts. The examples discussed here support what we hope is a useful overarching insight into the frontier challenges that remain to be addressed in future work to realize translations in technology or enabled new areas of science that would be truly transformational. New advances as might be made in the varying means of 4D fabrication—having highlighted here several general approaches based on additive and assembly based means of 4D patterning for functional integration—and the enabling materials that support them will unquestionably and in an enduring sense continue to drive important forms of progress in material research. The remarkable and accelerating reach of the work described in the current literature strongly argues this point as well as any metric might.

Still, there remains in our view a correlated opportunity to deeply think through and innovate within the chemistry of soft material composites and within 4D fabrication methods to progress this field beyond current capabilities. To that end, we want to offer specific challenges and opportunities currently within this field.

8.1. Integrating Materials of Diverse Properties and Sizes into Highly Functional Devices

In natural systems, soft responsive structural elements and chemistries are often integrated seamlessly with other structures of much different mechanical, chemical, and even optical properties. To give just a few common examples, consider the muscular–skeletal system and the lens and iris of the eye and associated musculature. It is the integration of soft(er) and hard(er) sub-elements, dynamic and responsive chemistries, and feedback systems (see an expanded discussion in Section 8.3), across many length scales, that gives the organism properties or functions that we are still just beginning to understand how to mimic in synthetic systems. When developing new 4D fabrication methods, we have little idea how to integrate sensing, mechanical elements, actuating element, and feedback directly into the final structures. Rather we tend to build independent subelements, and then utilize external engineering systems connected by wires or other elements. Topics such as multimaterial 3D printing, compliant electronics, autonomous feedback systems are all promising directions to explore hand-in-hand with innovations in 4D fabrication methods, however, this will only be the start to realize devices which match the functionality of even simple biological systems.

8.2. Development of Thermodynamically Efficient Stimuli-Responsive Chemistries

The mechanisms that drive responsive soft material chemistries are inherently inefficient when it comes to converting the energy of the stimulus to mechanical work. Much of this energy is lost as other forms of energy (e.g., heat, chemical reactions, etc.). When efficiency is measured in these systems,[102] it is often less than 1% and far below the thermodynamic efficiency of a simple electric motor. This inefficiency dramatically limits the classes of applications possible using responsive

soft chemistries either used in 4D fabrication methods or by 4D structures themselves.[127] It remains a grand challenge to develop soft chemistries that efficiently convert a stimulus' energy to mechanical work. Targeting chemistries where the energy of the stimulus goes directly toward changing the mechanical properties of the system, whether that be initiating a phase change within the material, or breaking or making chemical bonds, has potential to produce more efficient actuators than current approaches, where the majority of the input energy goes into, for example, changing the temperature of a material, and only a tiny fraction of the input energy goes into doing mechanical work.

8.3. Development of Sensory Feedback Mechanisms within Responsive Materials

One key aspect that defines most living organisms is their ability to use and integrate inputs from their local environment and respond accordingly. Although there has been a recent push toward developing synthetic systems which can sense and respond,[128] such capabilities remain largely absent in 4D fabricated structures. A significant opportunity in this space would be to develop soft architectures capable of taking external stimuli as inputs and providing logical output(s) as a response.

In conclusion, in such diverse fields as medicine, soft robotics, unconventional form factor electronics, the ability to construct complex 3D structural forms of materials which can respond, actuate, and even evolve into different shapes based on their environment will enable such materials to provide greatly enhanced functional properties. Developing important but heretofore difficult-to-realize forms of matter with such advanced system level properties will require a sustained and accelerating pace of progress in material chemistries of all forms. The current perspective highlights one avenue of such progress, that of the interplay of 3D and 4D designs for materials as one way to engender capacities to integrate soft materials in biomimetic and biologically compliant ways. While the examples and discussion here are hopefully a useful illustration, there is little doubt that there remain considerable opportunities to realize more impactful forms of progress, most notably in developing more sophisticated approaches to controlling the temporal evolution of a soft material structure's functional properties in response to the local environment. The latter aspiration is one we hope to address more meaningfully in future studies.

Acknowledgements

The authors gratefully thank the Army Research Office MURI (Grant No. W911NF-17-1-0351) for their support of this work. The authors thank Dr. Brittany Rauzan for assistance with this paper.

Conflict of Interest

The authors declare no conflict of interest.

Keywords

3D printing, 4D fabrication, biocompliant design, biomimetic design, directed assembly

Received: October 19, 2021
Revised: January 8, 2022
Published online: March 1, 2022

[1] F. Momeni, S. M. M. Hassani N, X. Liu, J. Ni, *Mater. Des.* **2017**, *122*, 42.
[2] X. Kuang, D. J. Roach, J. Wu, C. M. Hamel, Z. Ding, T. Wang, M. L. Dunn, H. J. Qi, *Adv. Funct. Mater.* **2019**, *29*, 1805290.
[3] M. Champeau, D. A. Heinze, T. N. Viana, E. R. de Souza, A. C. Chinellato, S. Titotto, *Adv. Funct. Mater.* **2020**, *30*, 1910606.
[4] M. Rafiee, R. D. Farahani, D. Therriault, *Adv. Sci.* **2020**, *7*, 1902307.
[5] A. Subash, B. Kandasubramanian, *Eur. Polym. J.* **2020**, *134*, 109771.
[6] N. Bowden, S. Brittain, A. G. Evans, J. W. Hutchinson, G. M. Whitesides, *Nature* **1998**, *393*, 146.
[7] a) J. Genzer, J. Groenewold, *Soft Matter* **2006**, *2*, 310; b) L. Ma, L. He, Y. Ni, *J. Appl. Phys.* **2020**, *127*, 111101.
[8] S. Cai, D. Breid, A. J. Crosby, Z. Suo, J. W. Hutchinson, *J. Mech. Phys. Solids* **2011**, *59*, 1094.
[9] a) J. Genzer, K. Efimenko, *Science* **2000**, *290*, 2130; b) D. Rhee, W.-K. Lee, T. W. Odom, *Angew. Chem., Int. Ed.* **2017**, *56*, 6523.
[10] J. M. Taylor, C. Argyropoulos, S. A. Morin, *Adv. Mater.* **2016**, *28*, 2595.
[11] a) S. P. Lacour, S. Wagner, Z. Huang, Z. Suo, *Appl. Phys. Lett.* **2003**, *82*, 2404; b) M. L. Hammock, A. Chortos, B. C.-K. Tee, J. B.-H. Tok, Z. Bao, *Adv. Mater.* **2013**, *25*, 5997; c) J. Zang, S. Ryu, N. Pugno, Q. Wang, Q. Tu, M. J. Buehler, X. Zhao, *Nat. Mater.* **2013**, *12*, 321.
[12] a) L. Ionov, *Soft Matter* **2011**, *7*, 6786; b) Z. Liu, A. Cui, J. Li, C. Gu, *Adv. Mater.* **2019**, *31*, 1802211; c) E. A. Peraza-Hernandez, D. J. Hartl, R. J. Malak, D. C. Lagoudas, *Smart Mater. Struct.* **2014**, *23*, 094001.
[13] a) L. Ionov, *Adv. Funct. Mater.* **2013**, *23*, 4555; b) Q. Ge, C. K. Dunn, H. J. Qi, M. L. Dunn, *Smart Mater. Struct.* **2014**, *23*, 094007; c) S. Felton, M. Tolley, E. Demaine, D. Rus, R. Wood, *Science* **2014**, *345*, 644; d) Y. Liu, J. Genzer, M. D. Dickey, *Prog. Polym. Sci.* **2016**, *52*, 79; e) J. T. B. Overvelde, T. A. de Jong, Y. Shevchenko, S. A. Becerra, G. M. Whitesides, J. C. Weaver, C. Hoberman, K. Bertoldi, *Nat. Commun.* **2016**, *7*, 10929.
[14] a) J. Guan, H. He, D. J. Hansford, L. J. Lee, *J. Phys. Chem.* **2005**, *109*, 23134; b) G. Stoychev, S. Zakharchenko, S. Turcaud, J. W. C. Dunlop, L. Ionov, *ACS Nano* **2012**, *6*, 3925; c) G. Stoychev, N. Puretskiy, L. Ionov, *Soft Matter* **2011**, *7*, 3277.
[15] A. M. Abdullah, X. Li, P. V. Braun, J. A. Rogers, K. J. Hsia, *Adv. Mater.* **2018**, *30*, 1801669.
[16] a) E. Palleau, D. Morales, M. D. Dickey, O. D. Velev, *Nat. Commun.* **2013**, *4*, 2257; b) C. Yoon, R. Xiao, J. Park, J. Cha, T. D. Nguyen, D. H. Gracias, *Smart Mater. Struct.* **2014**, *23*, 094008; c) J. Ryu, M. D'Amato, X. Cui, K. N. Long, H. J. Qi, M. L. Dunn, *Appl. Phys. Lett.* **2012**, *100*, 161908.
[17] Y. Liu, J. K. Boyles, J. Genzer, M. D. Dickey, *Soft Matter* **2012**, *8*, 1764.
[18] a) J. Deng, X. Lu, L. Liu, L. Zhang, O. G. Schmidt, *Adv. Energy Mater.* **2016**, *6*, 1600797; b) C. Xu, X. Wu, G. Huang, Y. Mei, *Adv. Mater. Technol.* **2019**, *4*, 1800486.
[19] a) M. Jamal, S. S. Kadam, R. Xiao, F. Jivan, T.-M. Onn, R. Fernandes, T. D. Nguyen, D. H. Gracias, *Adv. Healthcare Mater.* **2013**, *2*, 1142; b) V. A. Bolaños Quiñones, H. Zhu, A. A. Solovev, Y. Mei, D. H. Gracias, *Adv. Biosyst.* **2018**, *2*, 1800230.
[20] a) D. Rus, M. T. Tolley, *Nature* **2015**, *521*, 467; b) P. Polygerinos, N. Correll, S. A. Morin, B. Mosadegh, C. D. Onal, K. Petersen,

M. Cianchetti, M. T. Tolley, R. F. Shepherd, *Adv. Eng. Mater.* **2017**, *19*, 1700016; c) R. F. Shepherd, F. Ilievski, W. Choi, S. A. Morin, A. A. Stokes, A. D. Mazzeo, X. Chen, M. Wang, G. M. Whitesides, *Proc. Natl. Acad. Sci. USA* **2011**, *108*, 20400; d) P. Polygerinos, Z. Wang, K. C. Galloway, R. J. Wood, C. J. Walsh, *Rob. Autom. Syst.* **2015**, *73*, 135; e) F. Ilievski, A. D. Mazzeo, R. F. Shepherd, X. Chen, G. M. Whitesides, *Angew. Chem., Int. Ed.* **2011**, *50*, 1890; f) A. Zolfagharian, S. Gharaie, J. Gregory, M. Bodaghi, A. Kaynak, S. Nahavandi, *Soft Rob.* **2021**, https://doi.org/10.1089/soro.2020.0194.

[21] a) D. Liu, W. Chen, K. Sun, K. Deng, W. Zhang, Z. Wang, X. Jiang, *Angew. Chem., Int. Ed.* **2011**, *50*, 4103; b) H. Zhao, S. Sen, T. Udayabhaskararao, M. Sawczyk, K. Kučanda, D. Manna, P. K. Kundu, J.-W. Lee, P. Král, R. Klajn, *Nat. Nanotechnol.* **2016**, *11*, 82; c) Z. Yang, J. Wei, Y. I. Sobolev, B. A. Grzybowski, *Nature* **2018**, *553*, 313; d) A. H. Gröschel, A. Walther, T. I. Löbling, F. H. Schacher, H. Schmalz, A. H. E. Müller, *Nature* **2013**, *503*, 247.

[22] a) M. Grzelczak, L. M. Liz-Marzán, R. Klajn, *Chem. Soc. Rev.* **2019**, *48*, 1342; b) N. Krishnan, R. H. Fang, L. Zhang, *Adv. Drug Delivery Rev.* **2021**, *179*, 114006; c) N. R. Visaveliya, J. M. Köhler, *Adv. Funct. Mater.* **2021**, *31*, 2007407; d) J. Forth, P. Y. Kim, G. Xie, X. Liu, B. A. Helms, T. P. Russell, *Adv. Mater.* **2019**, *31*, 1806370.

[23] A. Zolfagharian, L. Durran, S. Gharaie, B. Rolfe, A. Kaynak, M. Bodaghi, *Sens. Actuators, A* **2021**, *328*, 112774.

[24] A. Zolfagharian, M. A. P. Mahmud, S. Gharaie, M. Bodaghi, A. Z. Kouzani, A. Kaynak, *Virtual Phys. Prototyping* **2020**, *15*, 373.

[25] S. Xu, Z. Yan, K.-I. Jang, W. Huang, H. Fu, J. Kim, Z. Wei, M. Flavin, J. McCracken, R. Wang, A. Badea, Y. Liu, D. Xiao, G. Zhou, J. Lee, H. U. Chung, H. Cheng, W. Ren, A. Banks, X. Li, U. Paik, R. G. Nuzzo, Y. Huang, Y. Zhang, J. A. Rogers, *Science* **2015**, *347*, 154.

[26] H. Zhao, K. Li, M. Han, F. Zhu, A. Vázquez-Guardado, P. Guo, Z. Xie, Y. Park, L. Chen, X. Wang, H. Luan, Y. Yang, H. Wang, C. Liang, Y. Xue, R. D. Schaller, D. Chanda, Y. Huang, Y. Zhang, J. A. Rogers, *Proc. Natl. Acad. Sci. USA* **2019**, *116*, 13239.

[27] a) X. Sun, L. Yue, L. Yu, H. Shao, X. Peng, K. Zhou, F. Demoly, R. Zhao, H. J. Qi, *Adv. Funct. Mater.* **2021**, https://doi.org/10.1002/adfm.202109805; b) A. Zolfagharian, A. Kaynak, A. Kouzani, *Mater. Des.* **2020**, *188*, 108411.

[28] R. L. Truby, J. A. Lewis, *Nature* **2016**, *540*, 371.

[29] M. Nadgorny, A. Ameli, *ACS Appl. Mater. Interfaces* **2018**, *10*, 17489.

[30] E. Yarali, M. Baniasadi, A. Zolfagharian, M. Chavoshi, F. Arefi, M. Hossain, A. Bastola, M. Ansari, A. Foyouzat, A. Dabbagh, M. Ebrahimi, M. J. Mirzaali, M. Bodaghi, *Appl. Mater. Today* **2022**, *26*, 101306.

[31] a) A. D. Valentine, T. A. Busbee, J. W. Boley, J. R. Raney, A. Chortos, A. Kotikian, J. D. Berrigan, M. F. Durstock, J. A. Lewis, *Adv. Mater.* **2017**, *29*, 1703817; b) M. Wei, F. Zhang, W. Wang, P. Alexandridis, C. Zhou, G. Wu, *J. Power Sources* **2017**, *354*, 134; c) T. V. Neumann, M. D. Dickey, *Adv. Mater. Technol.* **2020**, *5*, 2000070.

[32] a) J. T. Muth, D. M. Vogt, R. L. Truby, Y. Mengüç, D. B. Kolesky, R. J. Wood, J. A. Lewis, *Adv. Mater.* **2014**, *26*, 4415; b) Y. S. Rim, S.-H. Bae, H. Chen, N. De Marco, Y. Yang, *Adv. Mater.* **2016**, *28*, 4415.

[33] A. Kotikian, R. L. Truby, J. W. Boley, T. J. White, J. A. Lewis, *Adv. Mater.* **2018**, *30*, 1706164.

[34] R. L. Truby, M. Wehner, A. K. Grosskopf, D. M. Vogt, S. G. M. Uzel, R. J. Wood, J. A. Lewis, *Adv. Mater.* **2018**, *30*, 1706383.

[35] a) A. Kotikian, C. McMahan, E. C. Davidson, J. M. Muhammad, R. D. Weeks, C. Daraio, J. A. Lewis, *Sci. Rob.* **2019**, *4*, eaax7044; b) M. Wehner, R. L. Truby, D. J. Fitzgerald, B. Mosadegh, G. M. Whitesides, J. A. Lewis, R. J. Wood, *Nature* **2016**, *536*, 451; c) T. J. Wallin, J. Pikul, R. F. Shepherd, *Nat. Rev. Mater.* **2018**, *3*, 84.

[36] M. A. Skylar-Scott, J. Mueller, C. W. Visser, J. A. Lewis, *Nature* **2019**, *575*, 330.

[37] M. López-Valdeolivas, D. Liu, D. J. Broer, C. Sánchez-Somolinos, *Macromol. Rapid Commun.* **2018**, *39*, 1700710.

[38] a) D. B. Kolesky, K. A. Homan, M. A. Skylar-Scott, J. A. Lewis, *Proc. Natl. Acad. Sci. USA* **2016**, *113*, 3179; b) D. B. Kolesky, R. L. Truby, A. S. Gladman, T. A. Busbee, K. A. Homan, J. A. Lewis, *Adv. Mater.* **2014**, *26*, 3124; c) M. A. Skylar-Scott, S. G. M. Uzel, L. L. Nam, J. H. Ahrens, R. L. Truby, S. Damaraju, J. A. Lewis, *Sci. Adv.* **2019**, *5*, eaaw2459.

[39] a) A. I. M. Greer, E. Barbour, M. F. Cutiongco, J. M. Stormonth-Darling, N. Convery, R. E. Alsaigh, M. P. J. Lavery, N. Gadegaard, *Appl. Mater. Today* **2020**, *21*, 100782; b) D. A. Walker, J. L. Hedrick, C. A. Mirkin, *Science* **2019**, *366*, 360.

[40] T. Jungst, W. Smolan, K. Schacht, T. Scheibel, J. Groll, *Chem. Rev.* **2016**, *116*, 1496.

[41] a) A. Z. Nelson, K. S. Schweizer, B. M. Rauzan, R. G. Nuzzo, J. Vermant, R. H. Ewoldt, *Curr. Opin. Solid State Mater. Sci.* **2019**, *23*, 100758; b) M. E. Mackay, *J. Rheol.* **2018**, *62*, 1549.

[42] J. Li, C. Wu, P. K. Chu, M. Gelinsky, *Mater. Sci. Eng., R* **2020**, *140*, 100543.

[43] Z. Ding, C. Yuan, X. Peng, T. Wang, H. J. Qi, M. L. Dunn, *Sci. Adv.* **2017**, *3*, e1602890.

[44] D. Kokkinis, M. Schaffner, A. R. Studart, *Nat. Commun.* **2015**, *6*, 8643.

[45] C. Minas, D. Carnelli, E. Tervoort, A. R. Studart, *Adv. Mater.* **2016**, *28*, 9993.

[46] N. A. Sears, P. S. Dhavalikar, E. M. Cosgriff-Hernandez, *Macromol. Rapid Commun.* **2016**, *37*, 1369.

[47] a) B. M. Rauzan, A. Z. Nelson, S. E. Lehman, R. H. Ewoldt, R. G. Nuzzo, *Adv. Funct. Mater.* **2018**, *28*, 1707032; b) L.-y. Zhou, Q. Gao, J.-z. Fu, Q.-y. Chen, J.-p. Zhu, Y. Sun, Y. He, *ACS Appl. Mater. Interfaces* **2019**, *11*, 23573.

[48] a) A. Chortos, J. Mao, J. Mueller, E. Hajiesmaili, J. A. Lewis, D. R. Clarke, *Adv. Funct. Mater.* **2021**, *31*, 2010643; b) A. Kotikian, J. M. Morales, A. Lu, J. Mueller, Z. S. Davidson, J. W. Boley, J. A. Lewis, *Adv. Mater.* **2021**, *33*, 2101814; c) J. Mueller, J. R. Raney, K. Shea, J. A. Lewis, *Adv. Mater.* **2018**, *30*, 1705001; d) D. Liu, J. Ren, J. Wang, W. Xing, Q. Qian, H. Chen, N. Zhou, *J. Mater. Chem. C* **2020**, *8*, 15092; e) J. Zhao, H. Lu, Y. Zhang, S. Yu, O. I. Malyi, X. Zhao, L. Wang, H. Wang, J. Peng, X. Li, Y. Zhang, S. Chen, H. Pan, G. Xing, C. Lu, Y. Tang, X. Chen, *Sci. Adv.* **2021**, *7*, eabd6978.

[49] W. Liu, Y. S. Zhang, M. A. Heinrich, F. De Ferrari, H. L. Jang, S. M. Bakht, M. M. Alvarez, J. Yang, Y.-C. Li, G. Trujillo-de Santiago, A. K. Miri, K. Zhu, P. Khoshakhlagh, G. Prakash, H. Cheng, X. Guan, Z. Zhong, J. Ju, G. H. Zhu, X. Jin, S. R. Shin, M. R. Dokmeci, A. Khademhosseini, *Adv. Mater.* **2017**, *29*, 1604630.

[50] M. H. Ali, N. Mir-Nasiri, W. L. Ko, *Int. J. Adv. Manuf. Syst.* **2016**, *86*, 999.

[51] a) L. Sun, S. T. Parker, D. Syoji, X. Wang, J. A. Lewis, D. L. Kaplan, *Adv. Healthcare Mater.* **2012**, *1*, 729; b) C. M. González-Henríquez, M. A. Sarabia-Vallejos, J. Rodriguez-Hernandez, *Prog. Polym. Sci.* **2019**, *94*, 57.

[52] A. Sydney Gladman, E. A. Matsumoto, R. G. Nuzzo, L. Mahadevan, J. A. Lewis, *Nat. Mater.* **2016**, *15*, 413.

[53] J. W. Boley, W. M. van Rees, C. Lissandrello, M. N. Horenstein, R. L. Truby, A. Kotikian, J. A. Lewis, L. Mahadevan, *Proc. Natl. Acad. Sci. USA* **2019**, *116*, 20856.

[54] Y. Kim, H. Yuk, R. Zhao, S. A. Chester, X. Zhao, *Nature* **2018**, *558*, 274.

[55] C. P. Ambulo, J. J. Burroughs, J. M. Boothby, H. Kim, M. R. Shankar, T. H. Ware, *ACS Appl. Mater. Interfaces* **2017**, *9*, 37332.

[56] A. Nishiguchi, H. Zhang, S. Schweizerhof, M. F. Schulte, A. Mourran, M. Möller, *ACS Appl. Mater. Interfaces* **2020**, *12*, 12176.

[57] S. Naficy, R. Gately, R. GorkinIII, H. Xin, G. M. Spinks, *Macromol. Mater. Eng.* **2017**, *302*, 1600212.

[58] A. R. Rajkumar, K. Shanmugam, *J. Mater. Res.* **2018**, *33*, 4362.
[59] E. C. Davidson, A. Kotikian, S. C. Li, J. Aizenberg, J. A. Lewis, *Adv. Mater.* **2020**, *32*, 1905682.
[60] C. Li, A. Iscen, H. Sai, K. Sato, N. A. Sather, S. M. Chin, Z. Alvarez, L. C. Palmer, G. C. Schatz, S. I. Stupp, *Nat. Mater.* **2020**, *19*, 900.
[61] M. Nadgorny, Z. Xiao, C. Chen, L. A. Connal, *ACS Appl. Mater. Interfaces* **2016**, *8*, 28946.
[62] C. I. Gioumouxouzis, E. Tzimtzimis, O. L. Katsamenis, A. Dourou, C. Markopoulou, N. Bouropoulos, D. Tzetzis, D. G. Fatouros, *Eur. J. Pharm. Sci.* **2020**, *143*, 105176.
[63] a) M. R. O'Neill, E. Acome, S. Bakarich, S. K. Mitchell, J. Timko, C. Keplinger, R. F. Shepherd, *Adv. Funct. Mater.* **2020**, *30*, 2005244; b) C. Ladd, J.-H. So, J. Muth, M. D. Dickey, *Adv. Mater.* **2013**, *25*, 5081.
[64] J. M. McCracken, B. M. Rauzan, J. C. E. Kjellman, H. Su, S. A. Rogers, R. G. Nuzzo, *Adv. Funct. Mater.* **2019**, *29*, 1806723.
[65] C. Wang, S. S. Rubakhin, M. J. Enright, J. V. Sweedler, R. G. Nuzzo, *Adv. Funct. Mater.* **2021**, *31*, 2010246.
[66] G. Siqueira, D. Kokkinis, R. Libanori, M. K. Hausmann, A. S. Gladman, A. Neels, P. Tingaut, T. Zimmermann, J. A. Lewis, A. R. Studart, *Adv. Funct. Mater.* **2017**, *27*, 1604619.
[67] Q. Ge, A. H. Sakhaei, H. Lee, C. K. Dunn, N. X. Fang, M. L. Dunn, *Sci. Rep.* **2016**, *6*, 31110.
[68] Q. Zhang, D. Yan, K. Zhang, G. Hu, *Sci. Rep.* **2015**, *5*, 8936.
[69] a) Z. Ding, O. Weeger, H. J. Qi, M. L. Dunn, *Mater. Des.* **2018**, *137*, 256; b) F. Zhang, L. Wang, Z. Zheng, Y. Liu, J. Leng, *Composites, Part A* **2019**, *125*, 105571.
[70] X. Kuang, K. Chen, C. K. Dunn, J. Wu, V. C. F. Li, H. J. Qi, *ACS Appl. Mater. Interfaces* **2018**, *10*, 7381.
[71] A. Y. Lee, J. An, C. K. Chua, *Eng. J.* **2017**, *3*, 663.
[72] a) N. Ashammakhi, S. Ahadian, F. Zengjie, K. Suthiwanich, F. Lorestani, G. Orive, S. Ostrovidov, A. Khademhosseini, *Biotechnol. J.* **2018**, *13*, 1800148; b) G. H. Yang, M. Yeo, Y. W. Koo, G. H. Kim, *Macromol. Biosci.* **2019**, *19*, 1800441.
[73] B. Gao, Q. Yang, X. Zhao, G. Jin, Y. Ma, F. Xu, *Trends Biotechnol.* **2016**, *34*, 746.
[74] a) Z. Wan, P. Zhang, Y. Liu, L. Lv, Y. Zhou, *Acta Biomater.* **2020**, *101*, 26; b) T. Agarwal, S. Y. Hann, I. Chiesa, H. Cui, N. Celikkin, S. Micalizzi, A. Barbetta, M. Costantini, T. Esworthy, L. G. Zhang, C. De Maria, T. K. Maiti, *J. Mater. Chem. B* **2021**, *9*, 7608.
[75] a) X. Ning, X. Wang, Y. Zhang, X. Yu, D. Choi, N. Zheng, D. S. Kim, Y. Huang, Y. Zhang, J. A. Rogers, *Adv. Mater. Interfaces* **2018**, *5*, 1800284; b) Y. Zhang, F. Zhang, Z. Yan, Q. Ma, X. Li, Y. Huang, J. A. Rogers, *Nat. Rev. Mater.* **2017**, *2*, 17019; c) C. Wang, B. Qi, M. Lin, Z. Zhang, M. Makihata, B. Liu, S. Zhou, Y.-h. Huang, H. Hu, Y. Gu, Y. Chen, Y. Lei, T. Lee, S. Chien, K.-I. Jang, E. B. Kistler, S. Xu, *Nat. Biomed. Eng.* **2021**, *5*, 749.
[76] J. M. McCracken, S. Xu, A. Badea, K.-I. Jang, Z. Yan, D. J. Wetzel, K. Nan, Q. Lin, M. Han, M. A. Anderson, J. W. Lee, Z. Wei, M. Pharr, R. Wang, J. Su, S. S. Rubakhin, J. V. Sweedler, J. A. Rogers, R. G. Nuzzo, *Adv. Biosyst.* **2017**, *1*, 1700068.
[77] C. Wang, C. Wang, Z. Huang, S. Xu, *Adv. Mater.* **2018**, *30*, 1801368.
[78] H. Luan, Q. Zhang, T.-L. Liu, X. Wang, S. Zhao, H. Wang, S. Yao, Y. Xue, J. W. Kwak, W. Bai, Y. Xu, M. Han, K. Li, Z. Li, X. Ni, J. Ye, D. Choi, Q. Yang, J.-H. Kim, S. Li, S. Chen, C. Wu, D. Lu, J.-K. Chang, Z. Xie, Y. Huang, J. A. Rogers, *Sci. Adv.* **2021**, *7*, eabj3686.
[79] H. Fu, K. Nan, W. Bai, W. Huang, K. Bai, L. Lu, C. Zhou, Y. Liu, F. Liu, J. Wang, M. Han, Z. Yan, H. Luan, Y. Zhang, Y. Zhang, J. Zhao, X. Cheng, M. Li, J. W. Lee, Y. Liu, D. Fang, X. Li, Y. Huang, Y. Zhang, J. A. Rogers, *Nat. Mater.* **2018**, *17*, 268.
[80] a) S. Yao, Y. Zhu, *Adv. Mater.* **2015**, *27*, 1480; b) W. Piyawattanametha, P. R. Patterson, D. Hah, H. Toshiyoshi, M. C. Wu, *J. Microelectromech. Syst.* **2005**, *14*, 1329.
[81] M. Han, H. Wang, Y. Yang, C. Liang, W. Bai, Z. Yan, H. Li, Y. Xue, X. Wang, B. Akar, H. Zhao, H. Luan, J. Lim, I. Kandela, G. A. Ameer, Y. Zhang, Y. Huang, J. A. Rogers, *Nat. Electron.* **2019**, *2*, 26.
[82] X. Wang, R. Feiner, H. Luan, Q. Zhang, S. Zhao, Y. Zhang, M. Han, Y. Li, R. Sun, H. Wang, T.-L. Liu, X. Guo, H. Oved, N. Noor, A. Shapira, Y. Zhang, Y. Huang, T. Dvir, J. A. Rogers, *Extreme Mech. Lett.* **2020**, *35*, 100634.
[83] Z. Yan, M. Han, Y. Shi, A. Badea, Y. Yang, A. Kulkarni, E. Hanson, M. E. Kandel, X. Wen, F. Zhang, Y. Luo, Q. Lin, H. Zhang, X. Guo, Y. Huang, K. Nan, S. Jia, A. W. Oraham, M. B. Mevis, J. Lim, X. Guo, M. Gao, W. Ryu, K. J. Yu, B. G. Nicolau, A. Petronico, S. S. Rubakhin, J. Lou, P. M. Ajayan, K. Thornton, *et al.*, *Proc. Natl. Acad. Sci. USA* **2017**, *114*, E9455.
[84] Y. Park, C. K. Franz, H. Ryu, H. Luan, K. Y. Cotton, J. U. Kim, T. S. Chung, S. Zhao, A. Vazquez-Guardado, D. S. Yang, K. Li, R. Avila, J. K. Phillips, M. J. Quezada, H. Jang, S. S. Kwak, S. M. Won, K. Kwon, H. Jeong, A. J. Bandodkar, M. Han, H. Zhao, G. R. Osher, H. Wang, K. Lee, Y. Zhang, Y. Huang, J. D. Finan, J. A. Rogers, *Sci. Adv.* **2021**, *7*, eabf9153.
[85] B. H. Kim, K. Li, J.-T. Kim, Y. Park, H. Jang, X. Wang, Z. Xie, S. M. Won, H.-J. Yoon, G. Lee, W. J. Jang, K. H. Lee, T. S. Chung, Y. H. Jung, S. Y. Heo, Y. Lee, J. Kim, T. Cai, Y. Kim, P. Prasopsukh, Y. Yu, X. Yu, R. Avila, H. Luan, H. Song, F. Zhu, Y. Zhao, L. Chen, S. H. Han, J. Kim, *et al.*, *Nature* **2021**, *597*, 503.
[86] S. Lim, H. Luan, S. Zhao, Y. Lee, Y. Zhang, Y. Huang, J. A. Rogers, J.-H. Ahn, *Adv. Mater.* **2020**, *32*, 2001303.
[87] Z. Yan, F. Zhang, F. Liu, M. Han, D. Ou, Y. Liu, Q. Lin, X. Guo, H. Fu, Z. Xie, M. Gao, Y. Huang, J. Kim, Y. Qiu, K. Nan, J. Kim, P. Gutruf, H. Luo, A. Zhao, K.-C. Hwang, Y. Huang, Y. Zhang, J. A. Rogers, *Sci. Adv.* **2016**, *2*, e1601014.
[88] Y. Park, H. Luan, K. Kwon, S. Zhao, D. Franklin, H. Wang, H. Zhao, W. Bai, J. U. Kim, W. Lu, J.-H. Kim, Y. Huang, Y. Zhang, J. A. Rogers, *Adv. Funct. Mater.* **2019**, *29*, 1903181.
[89] J. K. Park, K. Nan, H. Luan, N. Zheng, S. Zhao, H. Zhang, X. Cheng, H. Wang, K. Li, T. Xie, Y. Huang, Y. Zhang, S. Kim, J. A. Rogers, *Adv. Mater.* **2019**, *31*, 1905715.
[90] X. Wang, X. Guo, J. Ye, N. Zheng, P. Kohli, D. Choi, Y. Zhang, Z. Xie, Q. Zhang, H. Luan, K. Nan, B. H. Kim, Y. Xu, X. Shan, W. Bai, R. Sun, Z. Wang, H. Jang, F. Zhang, Y. Ma, Z. Xu, X. Feng, T. Xie, Y. Huang, Y. Zhang, J. A. Rogers, *Adv. Mater.* **2019**, *31*, 1805615.
[91] Y. Zhang, Z. Yan, K. Nan, D. Xiao, Y. Liu, H. Luan, H. Fu, X. Wang, Q. Yang, J. Wang, W. Ren, H. Si, F. Liu, L. Yang, H. Li, J. Wang, X. Guo, H. Luo, L. Wang, Y. Huang, J. A. Rogers, *Proc. Natl. Acad. Sci. USA* **2015**, *112*, 11757.
[92] C. Yu, Z. Duan, P. Yuan, Y. Li, Y. Su, X. Zhang, Y. Pan, L. L. Dai, R. G. Nuzzo, Y. Huang, H. Jiang, J. A. Rogers, *Adv. Mater.* **2013**, *25*, 1541.
[93] A. Bandyopadhyay, B. Heer, *Mater. Sci. Eng., R* **2018**, *129*, 1.
[94] J. O. Hardin, T. J. Ober, A. D. Valentine, J. A. Lewis, *Adv. Mater.* **2015**, *27*, 3279.
[95] G. X. Gu, C.-T. Chen, D. J. Richmond, M. J. Buehler, *Mater. Horiz.* **2018**, *5*, 939.
[96] M. Schaffner, J. A. Faber, L. Pianegonda, P. A. Rühs, F. Coulter, A. R. Studart, *Nat. Commun.* **2018**, *9*, 878.
[97] a) O. Bertrand, J.-F. Gohy, *Polym. Chem.* **2017**, *8*, 52; b) Y. Hao, J. Meng, S. Wang, *Chin. Chem. Lett.* **2017**, *28*, 2085; c) J.-K. Chen, C.-J. Chang, *Materials* **2014**, *7*, 805.
[98] S.-J. Jeon, A. W. Hauser, R. C. Hayward, *Acc. Chem. Res.* **2017**, *50*, 161.
[99] a) E. Wang, M. S. Desai, S.-W. Lee, *Nano Lett.* **2013**, *13*, 2826; b) H. Yang, W. R. Leow, T. Wang, J. Wang, J. Yu, K. He, D. Qi, C. Wan, X. Chen, *Adv. Mater.* **2017**, *29*, 1701627.
[100] a) Y. Y. Liu, B. Xu, S. T. Sun, J. Wei, L. M. Wu, Y. L. Yu, *Adv. Mater.* **2017**, *29*, 1604792; b) Y. L. Yu, M. Nakano, T. Ikeda, *Nature* **2003**, *425*, 145.

[101] C. Li, A. Iscen, L. C. Palmer, G. C. Schatz, S. I. Stupp, *J. Am. Chem. Soc.* **2020**, *142*, 8447.
[102] P. Yuan, J. M. McCracken, D. E. Gross, P. V. Braun, J. S. Moore, R. G. Nuzzo, *Soft Matter* **2017**, *13*, 7312.
[103] a) F. Amir, X. Li, M. C. Gruschka, N. D. Colley, L. Li, R. Li, H. R. Linder, S. A. Sell, J. C. Barnes, *Chem. Sci. J.* **2020**, *11*, 10910; b) K. P. Liles, A. F. Greene, M. K. Danielson, N. D. Colley, A. Wellen, J. M. Fisher, J. C. Barnes, *Macromol. Rapid Commun.* **2018**, *39*, 1700781.
[104] a) Y. Liu, B. Shaw, M. D. Dickey, J. Genzer, *Sci. Adv.* **2017**, *3*, e1602417; b) G. Stoychev, A. Kirillova, L. Ionov, *Adv. Opt. Mater.* **2019**, *7*, 1900067.
[105] E. S. Epstein, L. Martinetti, R. H. Kollarigowda, O. Carey-De La Torre, J. S. Moore, R. H. Ewoldt, P. V. Braun, *J. Am. Chem. Soc.* **2019**, *141*, 3597.
[106] D. R. Griffin, A. M. Kasko, *J. Am. Chem. Soc.* **2012**, *134*, 13103.
[107] a) P. M. Kharkar, K. L. Kiick, A. M. Kloxin, *Chem. Soc. Rev.* **2013**, *42*, 7335; b) A. M. Kloxin, A. M. Kasko, C. N. Salinas, K. S. Anseth, *Science* **2009**, *324*, 59; c) A. M. Kloxin, M. W. Tibbitt, A. M. Kasko, J. A. Fairbairn, K. S. Anseth, *Adv. Mater.* **2010**, *22*, 61; d) E. R. Ruskowitz, C. A. DeForest, *Nat. Rev. Mater.* **2018**, *3*, 17087.
[108] a) W. Shen, J. Zheng, Z. Zhou, D. Zhang, *Acta Biomater.* **2020**, *115*, 75; b) L. Yang, H. Tang, H. Sun, *Micromachines* **2018**, *9*, 296.
[109] P. J. LeValley, R. Neelarapu, B. P. Sutherland, S. Dasgupta, C. J. Kloxin, A. M. Kloxin, *J. Am. Chem. Soc.* **2020**, *142*, 4671.
[110] a) Y. Shi, V. X. Truong, K. Kulkarni, Y. Qu, G. P. Simon, R. L. Boyd, P. Perlmutter, T. Lithgow, J. S. Forsythe, *J. Mater. Chem. B* **2015**, *3*, 8771; b) A. Paul, A. Jana, S. Karthik, M. Bera, Y. Zhao, N. D. P. Singh, *J. Mater. Chem. B* **2016**, *4*, 521.
[111] C. A. DeForest, K. S. Anseth, *Annu. Rev. Chem. Biomol. Eng.* **2012**, *3*, 421.
[112] a) T. T. Lee, J. R. García, J. I. Paez, A. Singh, E. A. Phelps, S. Weis, Z. Shafiq, A. Shekaran, A. del Campo, A. J. García, *Nat. Mater.* **2015**, *14*, 352; b) H. Zhao, E. S. Sterner, E. B. Coughlin, P. Theato, *Macromolecules* **2012**, *45*, 1723.
[113] a) L. L. Wang, C. B. Highley, Y.-C. Yeh, J. H. Galarraga, S. Uman, J. A. Burdick, *J. Biomed. Mater. Res., Part A* **2018**, *106*, 865; b) M. W. Tibbitt, K. S. Anseth, *Biotechnol. Bioeng.* **2009**, *103*, 655.
[114] A. De Mori, M. Peña Fernández, G. Blunn, G. Tozzi, M. Roldo, *Polymer* **2018**, *10*, 285.
[115] Y. Ji, K. Ghosh, X. Z. Shu, B. Li, J. C. Sokolov, G. D. Prestwich, R. A. F. Clark, M. H. Rafailovich, *Biomaterials* **2006**, *27*, 3782.
[116] a) S. N. Jayasinghe, A. N. Qureshi, P. A. M. Eagles, *Small* **2006**, *2*, 216; b) J. He, X. Zhao, J. Chang, D. Li, *Small* **2017**, *13*, 1702626.
[117] J. Fukuda, A. Khademhosseini, Y. Yeo, X. Yang, J. Yeh, G. Eng, J. Blumling, C.-F. Wang, D. S. Kohane, R. Langer, *Biomaterials* **2006**, *27*, 5259.
[118] a) H. Lin, D. Zhang, P. G. Alexander, G. Yang, J. Tan, A. W.-M. Cheng, R. S. Tuan, *Biomaterials* **2013**, *34*, 331; b) Z. Wang, R. Abdulla, B. Parker, R. Samanipour, S. Ghosh, K. Kim, *Biofabrication* **2015**, *7*, 045009.
[119] a) P. Eiselt, J. Yeh, R. K. Latvala, L. D. Shea, D. J. Mooney, *Biomaterials* **2000**, *21*, 1921; b) S. Sultan, A. P. Mathew, *Nanoscale* **2018**, *10*, 4421; c) T.-S. Jang, H.-D. Jung, H. M. Pan, W. T. Han, S. Chen, J. Song, *Int. J. Bioprint.* **2018**, *4*, 126.
[120] A. Badea, J. M. McCracken, E. G. Tillmaand, M. E. Kandel, A. W. Oraham, M. B. Mevis, S. S. Rubakhin, G. Popescu, J. V. Sweedler, R. G. Nuzzo, *ACS Appl. Mater. Interfaces* **2017**, *9*, 30318.
[121] J. M. McCracken, A. Badea, M. E. Kandel, A. S. Gladman, D. J. Wetzel, G. Popescu, J. A. Lewis, R. G. Nuzzo, *Adv. Healthcare Mater.* **2016**, *5*, 990.
[122] J. M. McCracken, B. M. Rauzan, J. C. E. Kjellman, M. E. Kandel, Y. H. Liu, A. Badea, L. A. Miller, S. A. Rogers, G. Popescu, R. G. Nuzzo, *Adv. Healthcare Mater.* **2019**, *8*, 1800788.
[123] a) E. O. Bachtiar, O. Erol, M. Millrod, R. Tao, D. H. Gracias, L. H. Romer, S. H. Kang, *J. Mech. Behav. Biomed. Mater.* **2020**, *104*, 103649; b) M. Kesti, C. Eberhardt, G. Pagliccia, D. Kenkel, D. Grande, A. Boss, M. Zenobi-Wong, *Adv. Funct. Mater.* **2015**, *25*, 7406.
[124] a) H. Amani, H. Arzaghi, M. Bayandori, A. S. Dezfuli, H. Pazoki-Toroudi, A. Shafiee, L. Moradi, *Adv. Mater. Interfaces* **2019**, *6*, 1900572; b) S. Cai, C. Wu, W. Yang, W. Liang, H. Yu, L. Liu, *Nanotechnol. Rev.* **2020**, *9*, 971; c) Z. Ma, Z. Mao, C. Gao, *Colloids Surf., B* **2007**, *60*, 137.
[125] a) W. Sun, W. Liu, Z. Wu, H. Chen, *Macromol. Rapid Commun.* **2020**, *41*, 1900430; b) O. Neděla, P. Slepička, V. Švorčík, *Materials* **2017**, *10*, 1115; c) W. Cheng, X. Zeng, H. Chen, Z. Li, W. Zeng, L. Mei, Y. Zhao, *ACS Nano* **2019**, *13*, 8537.
[126] a) N. Yi, H. Cui, L. G. Zhang, H. Cheng, *Acta Biomater.* **2019**, *95*, 91; b) H. Wang, P. Sun, L. Yin, X. Sheng, *InfoMat* **2020**, *2*, 527.
[127] a) X. Ma, H. Tian, *Acc. Chem. Res.* **2014**, *47*, 1971; b) H. Sun, C. P. Kabb, M. B. Sims, B. S. Sumerlin, *Prog. Polym. Sci.* **2019**, *89*, 61.
[128] a) X. Zhang, S. Soh, *Adv. Mater.* **2017**, *29*, 1606483; b) C. El Helou, P. R. Buskohl, C. E. Tabor, R. L. Harne, *Nat. Commun.* **2021**, *12*, 1633.

Jay M. Taylor obtained his Ph.D. in chemistry at the University of Nebraska–Lincoln in 2019 under the supervision of Prof. Stephen Morin. He then became a Postdoctoral Fellow in the Department of Material Science and Engineering at the University of Illinois Urbana-Champaign under Paul V. Braun. His research interests focus on the synthesis, assembly, and modifications of functional soft polymers.

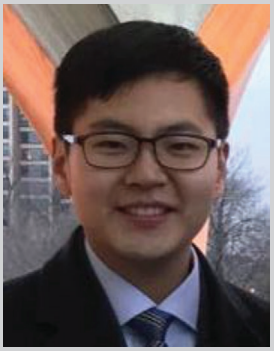

Haiwen Luan is a Postdoctoral Fellow in the Querrey Simpson Institute for Bioelectronics at Northwestern University, Evanston, IL, USA, under the supervision of John A. Rogers. He obtained his Ph.D. degree in mechanical engineering in 2019 from Northwestern University under the supervision of Prof. Yonggang Huang. His research interests focus on mechanically guided deterministic 3D assembly, and biointegrated flexible/stretchable electronics.

Jennifer A. Lewis is the Wyss Professor of Biologically Inspired Engineering and Director of the NSF Materials Research Science and Engineering Center at Harvard University. She is an elected member of the National Academy of Sciences, the National Academy of Engineering, the National Academy of Inventors, and the American Academy of Arts and Sciences.

John A. Rogers is the Louis Simpson and Kimberly Querrey Professor of Materials Science and Engineering, Biomedical Engineering, and Medicine at the Northwestern University, with affiliate appointments in Mechanical Engineering, Electrical and Computer Engineering, and Chemistry, where he is also Director of the recently endowed Querrey Simpson Institute for Bioelectronics. He is a member of the National Academy of Engineering, the National Academy of Sciences, the National Academy of Medicine, the National Academy of Inventors, and the American Academy of Arts and Sciences.

Ralph G. Nuzzo is the G. L. Clark Professor of Chemistry Emeritus at the University of Illinois Urbana-Champaign, with affiliate appointments at The California Institute of Technology and the KTH Royal Institute of Technology. He is a member of the National Academy of Sciences and the American Academy of Arts and Sciences.

Paul V. Braun is the Grainger Distinguished Chair in Engineering, the Director of the Illinois Materials Research Laboratory, and Professor of Materials Science and Engineering at the University of Illinois Urbana-Champaign. He received a Beckman Young Investigator Award, the Robert Lansing Hardy Award from TMS, and the Friedrich Wilhelm Bessel Research Award of the Alexander von Humboldt Foundation. He is an elected Fellow of the Materials Research Society and the American Association for the Advancement of Science.